의학박사 학위논문

Near-infrared imaging system for the detection of sentinel lymph node using indocyanine green and pullulan nanoparticle fluorescent tracers in large animal models

대동물에서 인도시아닌그린 및 플루란 나노입자 형광 표지자와 근적외선 촬영 장치를 이용한 감시림프절 영상

2013 년 2 월

서울대학교 대학원

의학과 박사과정

공 성 호

A thesis of the Degree of Doctor of Philosophy

대동물에서 인도시아닌그린 및 플루란 나노입자 형광 표지자와 근적외선 촬영 장치를 이용한 감시림프절 영상

Near-infrared imaging system for the detection of sentinel lymph node using indocyanine green and pullulan nanoparticle fluorescent tracers in large animal models

February 2013

The Department of Surgery,
Seoul National University
College of Medicine
Seong-Ho Kong

대동물에서 인도시아닌그린 및 플루란 나노입자 형광 표지자와 근적외선 촬영 장치를 이용한 감시림프절 영상

지도교수 양 한 광

이 논문을 의학박사 학위논문으로 제출함

2012 년 12 월

서울대학교 대학원
의학과 외과학 전공
공 성 호

공성호의 의학박사 학위논문을 인준함

2012 년 12 월

위 원 장 (인)

부위원장 (인)

위 원 (인)

위 원 (인)

위 원 (인)

Near-infrared imaging system for the detection of sentinel lymph node using indocyanine green and pullulan nanoparticle fluorescent tracers in large animal models

by

Seong-Ho Kong

A thesis submitted to the Department of Surgery in partial fulfillment of the requirement of the Degree of Doctor of Philosophy in Surgery at Seoul National University College of Medicine

December 2012

Approved by Thesis Committee:

Professor _____Chairman

Professor _____Vice chairman

Professor _____

Professor _____

Professor _____

ABSTRACT

Introduction: The near-infrared (NIR) imaging system has been applied for the sentinel lymph node biopsy with a potential to overcome the limitation of current techniques. The purpose of this study was to design the NIR tracers and the large animal models, to develop and assess the NIR tracers for the clinical application in sentinel lymph node mapping in human malignant tumors.

Methods: A new near-infrared-emitting polymer nanogel (NIR-PNG) was developed by conjugating IRDye800 organic dye to biodegradable pullulan-cholesterol polymer nanogels. Breast cancer, cutaneous malignancy, small intestine, and gastric cancer models were prepared using 40kgs of female pigs and 30kgs of female dogs. Indocyanine green (ICG), ICG/poly ɣ-glutamic acid(PGA) complex, ICG/hyaluronic acid(HA) mixture, and IRDye900-conjugated pullulan-cholesterol nanoprobe (NIR-PNG) were examined in different concentrations and dosages to assess the characteristics of tracers such as sensitivity, pattern of dispersion, and retention time using NIR imaging system.

Results: The NIR-PNG nanoprobes had about 30nm's diameter. It was more photostable and had higher signal intensity and longer retention time in the lymph node compared with those of IRDye800-free dye when injected into the front paw of mice. Breast cancer model in pigs were not a proper model because of unpredictable lymphatic flows. Breast and inguinal model in dogs and inguinal and small bowel model in pigs were found to be useful with highly sensitive NIR images of not only the sentinel lymph nodes but also lymphatic flows, however, they were not useful in examine the lymphatic

flows after the sentinel nodes. A gastric cancer model to examine the movement of tracers from the lower body greater curvature side of the stomach via the infrapyloric nodes and to suprapancreatic nodes was useful to assess lymphatic flows after the sentinel nodes. NIR-PNG seemed to be the best candidate for NIR tracers with the highest selective to show only one sentinel lymph node and prolonged retention time, in contrast to dilute ICG and ICG/PGA complex that spread multi-directionally to numerous lymph nodes and beyond the sentinel nodes, although they could be also useful tracers to show the detailed lymphatic flows with high sensitivity. ICG and ICG/HA mixture showed applicability of endoscopic injection in marking method for early gastric cancer to localize the tumor and decide the resection line in gastrectomy

Conclusions: NIR imaging system may provide superior visual sensitivity in sentinel lymph node biopsy for numerous malignancies. NIR-PNG, the best candidate, and also diluted ICG and ICG/PGA complex can be useful for sentinel node mapping of gastric cancer compared with conventional vital dye method using ICG in high concentration.

*This work about development of NIR-PNG was published in ACS Nano (Noh YW, Kong SH (co-first author), Choi DY, et al. Near-infrared emitting polymer nanogels for efficient sentinel lymph node mapping. ACS Nano. 2012 Sep 25;6(9):7820-31.[1])

Keywords: Sentinel lymph node, near-infrared imaging, large animal

Student number: 2009-30497

CONTENTS

LIST OF TABLES AND FIGURES

Chapter 1

Chapter 2

Chapter 3

LIST OF ABBREVIATIONS

DLS: dynamic light scattering

HA: hyaluronic acid

ICG: Indocyanine green

NIR: near-infrared

NIR-PNG: near-infrared-emitting polymer nanogel

PGA: poly ɣ-glutamic acid

SNL: sentinel lymph node

TEM: transmission electron microscope

GENERAL INTRODUCTION

A sentinel lymph node navigation surgery, a method to decide whether to do lymphadenectomy using an intraoperative pathologic examination of the lymph node that receives lymphatic flows from the malignancy directly, has been proven to be effective and used for breast cancer and malignant melanoma.[2,3] The sentinel lymph node navigation surgery has been also studied for early gastric cancer to avoid unnecessary extensive lymph node dissection and apply tailored surgical extent to each individual, although it has not become a standard method due to complex lymphatic structure around the stomach and significant false negativity.[4] The most commonly used tracers for sentinel node mapping are vital dyes such as patent blue, isosulfan blue, or Indocyanine green (ICG), which are detected by visual inspection, and radioisotopes conjugated with colloid particles, which are detected by gamma probes yielding audible signals.[5-8] In gastric cancer, low sensitivity and rapid dispersion of vital dyes, and the need for strict radio hazard-proof protocols and the invisibility of radioisotopes have been recognized as limitations.[9]

The near-infrared (NIR) imaging system using the wavelength between 700 and 1000 nm has been found to be advantageous for *in vivo* imaging due to reduced optical scattering and low tissue autofluorescence, resulting in a high signal-to-background ratio and a significant imaging depth. [10,11] It has been suggested for sentinel lymph node mapping as a highly sensitive visible method without the concern for radio-hazard. A vital dye ICG also produces near-infrared fluorescence and has been tried to be applied for sentinel node mapping of several cancers such as breast,[12-14] colon,[15,16] and vulva cancer.[17] However, the size of the ICG is too small for sentinel node mapping because it is free particle, resulting in too rapid and extensive dispersion in sentinel node mapping using NIR imaging, too.

In this study, we purposed to develop clinically applicable NIR imaging systems for sentinel lymph node mapping in various cancers by designing new tracers and large animal models to assess the tracers. Especially we compared newly developed tracers including near-infrared-emitting polymer nanogel (NIR-PNG) in a gastric cancer model to find the best tracer for sentinel node mapping. We also tried to apply the system as a localization method for early gastric cancer.

CHAPTER 1

Development of new NIR tracers

INTRODUCTION

As NIR producing fluorophores, inorganic fluorescent semiconductor nanocrystals which is also called “quantum dots” have been proposed as good tracers with very high quantum yields, liable capability of tuning the wavelenth, and remarkable resistance to photobleaching. However, the quantum dots could not be readily applied to human because they used potentially toxic materials such as cadmium, tellurium, selenium, and lead for a core, which are worrisome even though the dosage used for imaging is usually far less than those known to be toxic.[18-21] In contrast, organic fluorophores including indocyanine green and modified heptamethine indocyanines have disadvantage of lower quantum yields and high susceptibility to photobleaching, but have better safety profiles. Especially, ICG was approved for use in indicator-dilution studies by FDA in 1958, and known to be one of the least toxic agents ever administered to humans, with the only known adverse reaction being rare anaphylaxis.[22] However, When ICG is used in the same concentration for visual inspection in gastric cancer, the problems of rapid and extensive dispersion persist in NIR imaging system because of small size of particles.[23] To overcome these disadvantages of ICG and optimize NIR imaging method to clinical practice, three strategies could be considered: the first was to adjust the concentration of ICG, and the second was to physically mix ICG with adjunctive chemical to enhance the retention time of tracers in the sentinel lymph nodes. Albumin and hyaluronic acid has been used by some investigators,[24-26] and the poly ɣ-glutamic acid (ɣ-PGA) has been reported higher signal intensity and longer retention time in the sentinel lymph node in small animal models by the collaborative researcher of this study.[27] The last strategy was to compose a nanoparticle in an optimal size (5-50nm) for sentinel lymph node mapping. [28-30] Pullulan, a neutral linear polysaccharide produced from starch by *Aureobasidium pullulans*, was used

for this study because it has been extensively studied for applications in biomedical field due to its water soluble, biodegradable, nontoxic, and nonimmunogenic properties, as well as its amenability to chemically modification.[31]

In this study, we tried to find the optimal concentration of ICG using pig models and examine the properties of newly developed near-infrared-emitting polymer nanogel (NIR-PNG)

MATERIALS AND METHODS

1. ICG and ICG/ ɣ -PGA complex

Indocyanine green (Mw = 744, Dongindang Pharmaceutical, Siheung, Korea) and Poly ɣ-glutamic acid (Mw= 50 and 5,000 kDm, BioLeaders Corporation, Daejeon, Korea) were used in the study. The ICG/ ɣ -PGA complex was prepared in an aqueous solution according to the same manner in the previous study,[27] by mixing ICG (0.01mg/ml) and ɣ-PGA (0.01, 0.1% (w/v)) in 1 ml of water under rapid vortexing at room temperature. (Figure 1-1) The spectra were normalized for the maximum absorbance (λab = 780 nm) and the maximum fluorescence (λem = 820 nm) of ICG. It has been reported that the fluorescence intensities of ICG/ ɣ -PGA complexes exhibited a much slower decrease with time compared to that of ICG at both 25°C and 37°C during 3 days of measurement of fluorescence emission spectra. A cytotoxic assay also has been performed on a dendritic cell line, which is one of the most abundantly present in the lymph node, by measuring the cell viability with a colorimetric MTT assay, and the ICG/ ɣ -PGA complex showed good dendritic cell viability identical to that of the control. The previous study also reported that the ICG/- ɣ PGA50 (0.1%) complex showed a much brighter NIR fluorescent signal of SLN in the axillary sentinel lymph node for longer duration compared with ICG when injected into the right paw of mice.

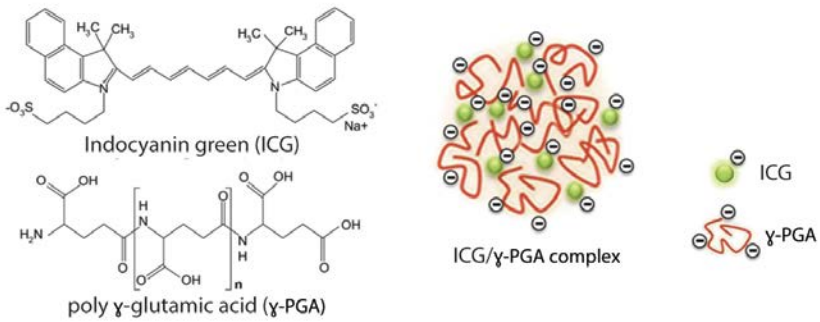

Figure 1-1. Structure of ICG, poly ɣ -PGA , ICG/ ɣ -PGA complex (courtesy by pf. Lim YT)

To find optimal concentration of ICG in intestinal tract, different concentrations of ICG were injected in the small bowel and the stomach of a pig. Under general anesthesia, the small bowel of a pig was exposed by a midline incision. 0.1ml of ICG (0.0001, 0.01, 0.1, 1 and 5mg/ml) was injected into the small bowel subserosally by 25 gauge needle and the fluorescence signals were observed using the NIR camera system. To simulate endoscopic submucosal injection into the stomach, the stomach was removed and opened along the greater curvature. 0.1ml of ICG (0.001, 0.01, 0.1, 1 and 5mg/ml) was injected in the submucosal layer by 25 gauge needle, and the opened greater curvature of the stomach was re-closed by a continuous suture. Fluorescence signals were observed with the NIR camera system with 4mmHg/ml of pressure maintained inside the stomach using a laparoscopic CO2 inflator to simulate a pressure effect of gastroscopy.

2. NIR-PNG

Preparation and Characterization of the NIR-PNG Nanoprobes

To synthesize NIR emitting polymer nanogels having a hydrodynamic diameter about 30 nm (Figure 1-2), which size is known to be optimal for lymph node uptake, pullulan (Wako Pure Chemicals, Tokyo, Japan) polymers were modified with the following three steps ; i) pullulan-cholesterol conjugate was synthesized by conjugating amine-cholesterol on pullulan, ii) amine moieties were additionally introduced for the conjugation of NIR emitting fluorophores, iii) NHS terminated IRDye800 (Li-COR, Lincoln, NE, USA) was finally conjugated with aminated pullulan-cholesterol conjugate. The size of the NIR-PNG nanoprobes was measured by dynamic light scattering (DLS) and transmission electron microscope (TEM). The amount of conjugated dye was estimated to be 10 μg of dye per 1 mg of NIR-PNG nanoprobes via UV_vis spectrophotometer (NEOSYS-2000, Sinco, Seoul,

Korea). The emission spectrum of NIR-PNG nanoprobes was compared to the spectrum of IRDye800-free dye dissolved in water at 25°C by a fluorescence spectrophotometer (LS 55, PerkinElmer Instruments, Wellesley, MA, USA) using an excitation wavelength of 775 nm and an emission range of 780-900 nm.

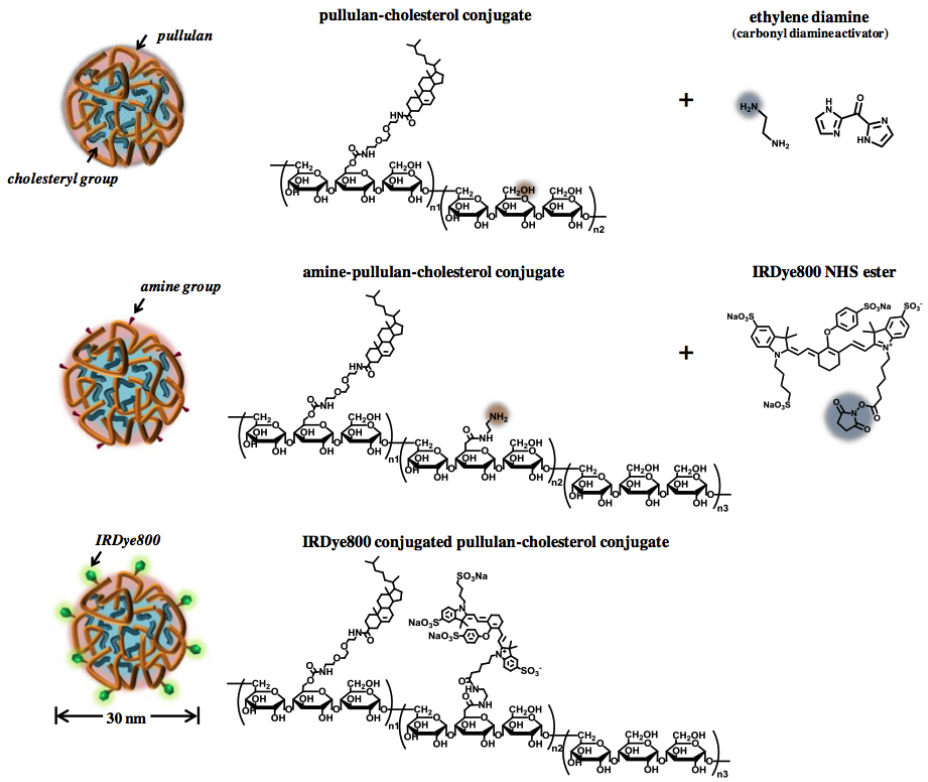

Figure 1-2. Synthetic scheme and chemical structure of NIR-PNG nanoprobes based on pullulan- cholesterol nanogel conjugated with IRDye800 organic dye.

In Vitro Cytotoxicity Assay

Cell cytotoxicity was measured by analyzing the cleavage of thiazoyl blue tetrazolium bromide (MTT; Sigma-Aldrich) by the succinate dehydrogenases of living cells to yield formazan. DC2.4 cells ($2x10^4$ cells/well), a dendtitic cells residing in the lymph nodes or the CT-26 ($2x10^4$ cells/well) murine epithelial colorectal adenoma cell line. They were seeded on a flat- bottomed

96-well plate (Corning Costar, Cambridge, MA, USA) in RPMI medium (Invitrogen, Grand Island, NY, USA) supplemented with 10% heat-inactivated fetal bovine serum (Invitrogen), $5x10^{-5}$ M 2-mercaptoethanol (Sigma-Aldrich), 50 IU/mL penicillin, and 50 mg/mL streptomycin (Invitrogen). After incubating the cells with various concentrations of the NIR-PNG nanoprobes and IRDye800 for 24-48 h, MTT (10 μL/well of a 5 mg/mL MTT stock solution in PBS) was directly added to each well, and the plates were incubated at 37°C for 4 h. A colorimetric MTT assay was conducted by adding dimethyl sulfoxide (DMSO; Sigma-Aldrich) to solubilize the formazan, and the absorbance was measured at 562 nm. To determine whether NIR-PNG nanoprobes have any effect on cytokine production of DC2.4 cells, the levels of IL-6 and TNF-R were also measured after incubation with NIR-PNG nanoprobes or IRDye800 for 24 h.

In Vivo SLN Mapping in a Small Animal

To evaluate the characteristics of NIR-PNG nanoprobes as the tracer for sentinel node mapping, NIR-PNG (50 μg of samples in 50 μL of water) and IRDye800 were intradermally injected into the right paw of the BALB/c mice that were anesthetized with 300 μL of a 2.5% avertin solution (2,2,2-tribromoethanol-tert-amyl alcohol, Sigma) and the imaging areas were treated with a depilatory cream. The axillary sentinel nodes were observed by NIR imaging system and taken out and observed by immunohistofluoresence microscopy. The distribution of tracers was observed with macrophages (CD68+ cell) or dendritic cells (CD205+ cell) stained by rat anti-mouse CD68 (F4/80, Serotec, Oxford, UK) and rat anti-mouse CD205 (DEC-205, Serotec) overnight at 4°C. *In vitro* cellular uptake was evaluated by incubating a murine dendritic cell line (DC2.4) with NIR-PNG nanoprobes and IRDye800 to confirm their characteristic to be phagocytosed by cells *in vivo* by

fluorescence microscope with lysosomes stained with a FITC-labeled lysosome-specific antibody (FITC-LAMP-1 antibody) and LysoTracker.

RESULTS

Optimal concentration for sentinel lymph node biopsy in the intestinal tract

In vitro NIR imaging of ICG in cryotubes showed the brightest fluorescence signal at the concentration of 0.01mg/ml. (Figure 1-3. A and B) When ICG was injected in the small bowel and the stomach, 0.01mg/ml of ICG seemed to be insufficient for the sentinel lymph node biopsy. ICG in 1 and 5mg/ml did not show bright signal *in vitro*, however when it was injected in the small bowel, it showed bright signal with a central dark central area, which was caused by a quenching effect. (Figure 1-3. C and D) The signals in the lymphatic vessels and the lymph nodes in the small bowel with these concentrations were identified in a delayed manner; the green color of the ICG was identified into the lymphatic system by naked eyes, then the diluted ICG showed bright NIR signal. The average size of the injection site of 1mg/ml and 5mg/ml of ICG was too large; 2.9cm and 3.7cm, respectively, compared with 1.7cm in 0.1mg/ml of ICG. Therefore, the optimal concentration of ICG seemed to be in between 0.1 and 1mg/ml, and 0.1mg/ml was chosen for the next experiments as the lowest and effective concentration for sentinel lymph node mapping.

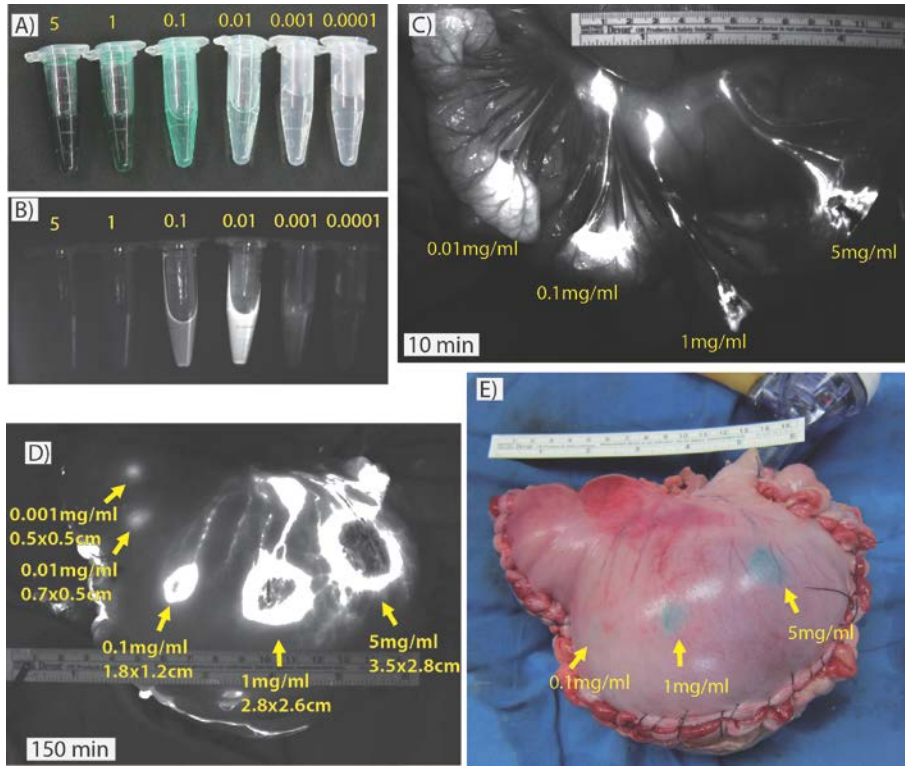

Figure 1-3. NIR images of ICG in different concentrations.
A) in vitro color of ICG (values are in mg/ml), B) in vitro NIR imaging of ICG in cryotubes (values are in mg/ml), C) in vivo NIR images in the small bowel 10 minutes after injection D) ex vivo NIR images in the stomach 150 minutes after injection, E) Color image of the stomach of pig. Concentration of ICG in 0.1mg/ml seemed to be the optimal concentration with the smallest signal size of injection site and good lymphatic flows with the least quenching effect.

Physicochemical properties of NIR-PNG

The size of the NIR-PNG nanoprobes was measured by dynamic light scattering (DLS), which revealed that the mean diameter was approximately 30 nm (Figure 1-4.A). The average size of these nanoprobes (n = 134) measured by TEM was found to be slightly smaller than those measured by DLS, possibly due to the air-drying process which causes the nanoprobes to shrink and attain a smaller size than under water. The zeta potentials of the NIR-PNG nanoprobes, which is initially -9.76±2.29mV, remarkably increased to 34.76±0.70 mV when the amine in introduce. It indicated that the negatively charged surface was converted to a positively charged surface.

The zeta potential decreased to 11.05±0.35 mV when the negatively charged IRDye800 dye is attached to the surface. Measurement of the amount of dye per milligram of NIR-PNG nanoprobes revealed that 1 mg of NIR-PNG nanoprobes conjugated approximately 10 μg of IRDye800.

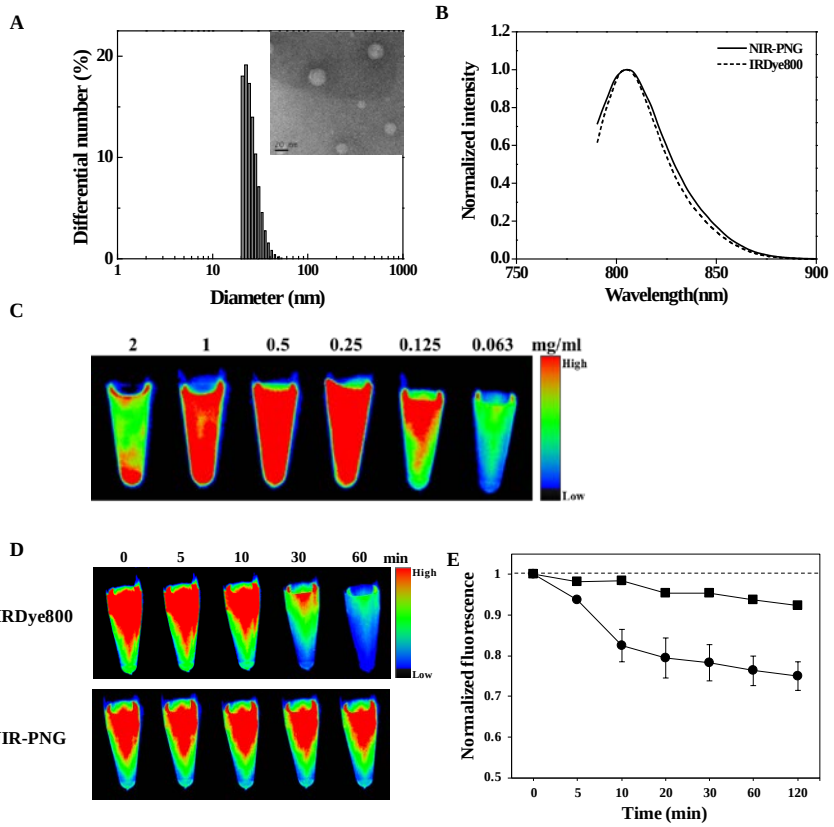

Figure 1-4. Physicochemical properties of NIR-PNG nanoprobes. (A) Size and size distribution of NIR-PNG nanoprobes measured by DLS and TEM (insert). The scale bar in the TEM image represents 20 nm. (B) Fluorescence spectra of NIR-PNG nanoprobes and IRDye800 dye. The spectra were normalized for the maximum fluorescence at 810 nm. (C) *In vitro* NIR fluorescence image (pseudo color) of the NIR-PNG nanoprobes in water according to the concentration of NIR-PNG nanoprobes. (D, E) Fluorescence stability of IRDye800 dye (1 μg/ml) and NIR-PNG nanoprobes (100 μg/ml, conjugated with 1 μg/ml IRDye800) were determined by using the NIR fluorescence images (D) and fluorescence maximum emission spectra (E) in water at room temperature over time (2 hr).

Optical Properties of NIR-PNG Nanoprobes

In a dissolved status in water at 25°C, the emission spectra of the IRDye800 and NIR-PNG nanoprobes were similar without spectral shift of NIR-PNG. (Figure 1-4 B). NIR fluorescence imaging was performed on serial dilutions (63 to 2000 μg/mL) of the NIR-PNG nanoprobes using a 785 nm LED light source and an 835/45 nm emission filter. The fluorescence intensity of NIR-PNG was highest at the concentration of 0.5 mg/mL, and the fluorescence signal decreased as the concentration was increased up to 1-2 mg/mL (Figure 1-4 C) During 2 hours in water at 25°C, the fluorescence intensity of the NIR-PNG nanoprobes did not decrease significantly over time, while fluorescence intensity of IRDye800 decreased (Figure 1-4 D, E).

Cytotoxicity of NIR-PNG Nanoprobes

NIR-PNG nanoprobes showed no cytotoxic effects toward both the DC2.4 (Figure 1-5 A) and CT-26 cell line (Figure 1-5 B) up to 100 μg/mL of concentration. As shown in Figure 1-6, the presence of nanoprobes did not alter cytokine levels, whereas dendritic cells (DCs) responded to LPS stimulation with a strong increase in cytokine production. In this analysis, we found that NIR-PNG nanoprobes did not affect production of the immune response-associated cytokines.

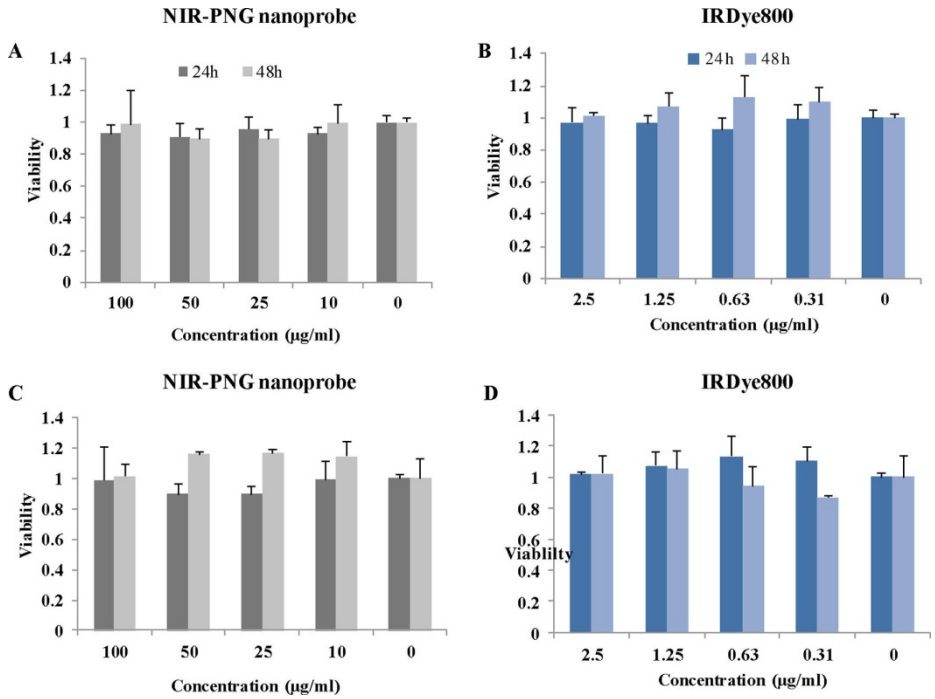

Figure 1-5. Cytotoxicity of the NIR-PNG nanoprobes. Cytotoxicities of the NIR-PNG nanoprobes (A and C) and IRDye800 (B and D) were determined for mouse DC2.4 cells (A and B) and CT-26 adenocarcinoma (C and D) after 24 and 48 h of incubation for each molecule at indicated concentrations.

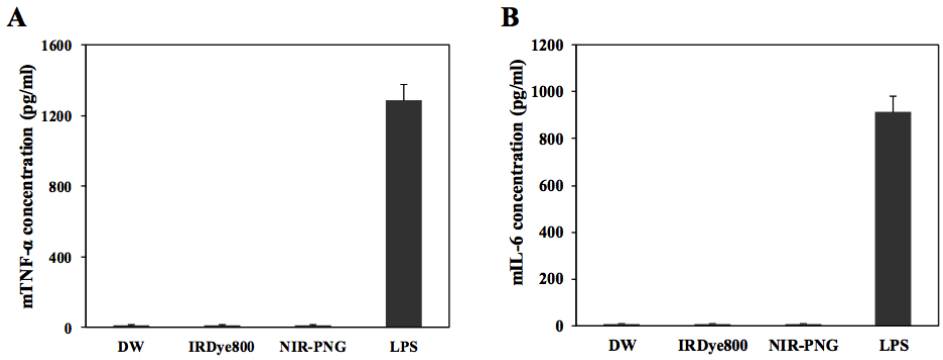

Figure 1-6. The effect of NIR-PNG on the cytokine production of DC2.4 cells. DC2.4 cells were treated with NIR-PNG (0.1 mg/ml), IRDye800 (2.5 μg/ml) or LPS (1μg/ml). After 24 h, supernatants were collected and analyzed by ELISA to measure the levels of TNF-α (A) and IL-6 (B) cytokines. The cytokine production of DC2.4 cells were not changed when treated with NIR-PNG. In contrast, the levels of cytokine production were enhanced by stimulation with LPS. Graphs represent the mean±SD of duplicates.

***In vivo* Sentinel node mapping in the right paw of mice**

The NIR- PNG nanoprobes (50 μg of samples in 50 μL of water) were intradermally injected into the right paw of a mouse and imaged for *in vivo* migration of NIR-PNG nanoprobes using a NIR optical imaging system. Compared with weak signal of IRDye800 in axillary LN of mice, which was resulted from easy passage of the dye through the SLN and diffusion into other lymph nodes due to small size of dye, the signal of NIR-PNG was much brighter over 2-30 min. (Figure 1-7) Methylene blue dye, one of the vital dyes used in sentinel node mapping as isosulfan blue, was injected in the same injection site after 30 minutes, and it indicated the same lymph node that the NIR-PNG indicated. The NIR fluorescence signals in the excised lymph node were associated with the SLN, but not the adjacent fat tissue, indicated preferential accumulation of the NIR-PNG nanoprobes in the SLN. The NIR-PNG nanoprobes were accumulated in the SLN to a greater extent than IRDye800 (Figure 1-7 C, D; IRDye800, G, H; NIR-PNG). The lymph node retention time of the NIR-PNG nanoprobes and IRDye800 measured at 1-48 h postinjection showed prolonged signal of NIR-PNG at 24 and 48h, but no signal of IRDye800 (Figure 1-7 I).

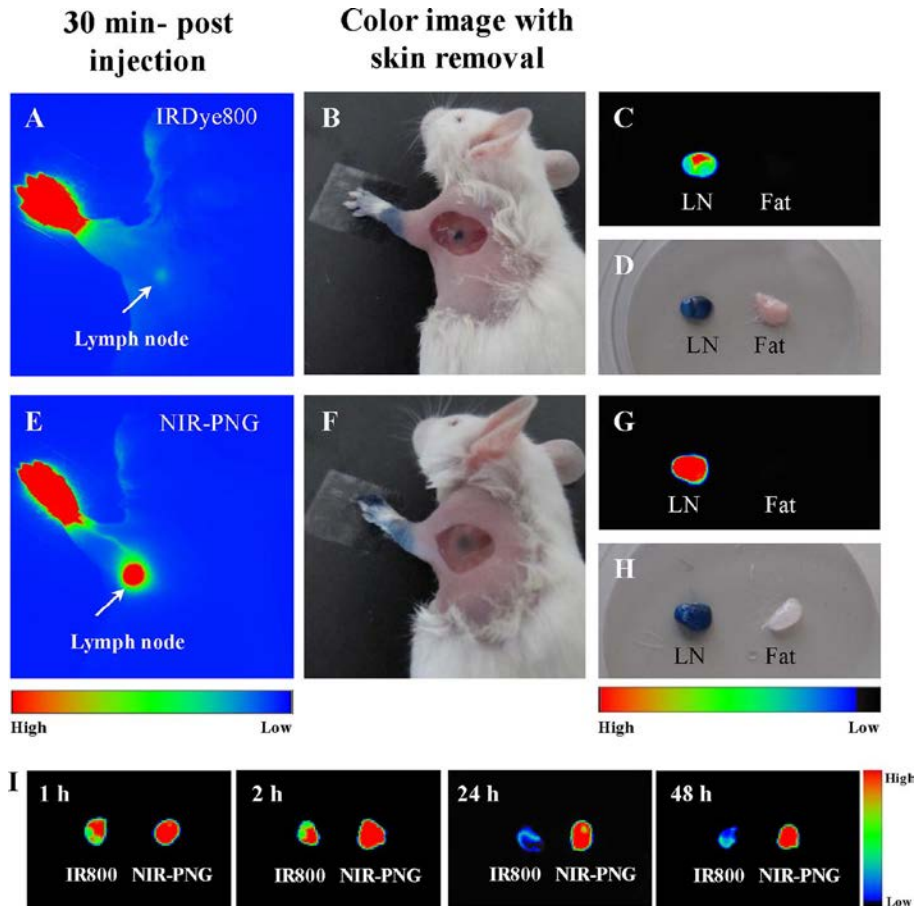

Figure 1-7. SLN mapping procedure with IRDye800 and NIR-PNG nanoprobes. (A, E) In vivo NIR fluorescence images (pseudocolor) at 30 min postinjection of the IRDye800 dye (0.5 μg in 50 μg of PBS) (A) and NIR-PNG nanoprobes (50 μg, conjugated with 0.5 μg of IRDye800, in 50 μg of PBS) (E). The arrows indicate the axillary SLN. (B, F) Color images of a mouse after methylene blue dye injection and skin removal after an injection of the IRDye800 (B) and NIR-PNG nanoprobes (F). (C_H) Ex vivo NIR fluorescence (C, G) and color (D, H) images of dissected LN and fat tissue of a mouse injected with the IRDye800 (C, D) and NIR-PNG nanoprobes (G, H). (I) Ex vivo NIR fluorescence images of dissected SLN on time points in the range 1_48 h postinjection.

Localization of NIR-PNG Nanoprobes within the SLN.

The immunohistofluorescence image of the SLN indicated good regional lymph node retention of the NIR-PNG nanoprobes at 30 min, whereas only a fraction of the IRDye800 was localized in the lymph node. (Figure 1-8) The IRDye800 was not localized in the subcapsular space with the macrophages ($CD68^+$ cell) (Figure 1-8 A, C) or dentritic cells ($CD205^+$ cell) (Figure 1-8 E). However, NIR-PNG nanoprobes were significantly co-localized with macrophages (Figure 1-8 B, D) or dendritic cells (Figure 1-8 F). Enlarged images showed that the fluorescence signals of the IRDye800 were located outside the cells (Figure 1-8 A, C and Figure 1-9 A, arrowhead). In contrast, many fluorescence signals of the NIR-PNG nanoprobes were located on the cell surface and inside the cells (Figure 1-8 B, D and Figure 1-9 B, arrow).

In vitro fluorescence microscope after incubating NIR-PNG ad IRDye800 reveal that the NIR-PNG nanoprobes were more efficiently taken up by DC2.4 cells than IRDye800 In vitro cellular uptake. In the dendritic cells, NIR-PNG were mainly colocalized with the signal of FITC-LAMP-1 anti-lysosomal antibody (Figure 1-10 C and Figure 1-11), indicating that internalized NIR-PNG nanoprobes preferentially localized in the lysosomal compartments of phagocytic cells.

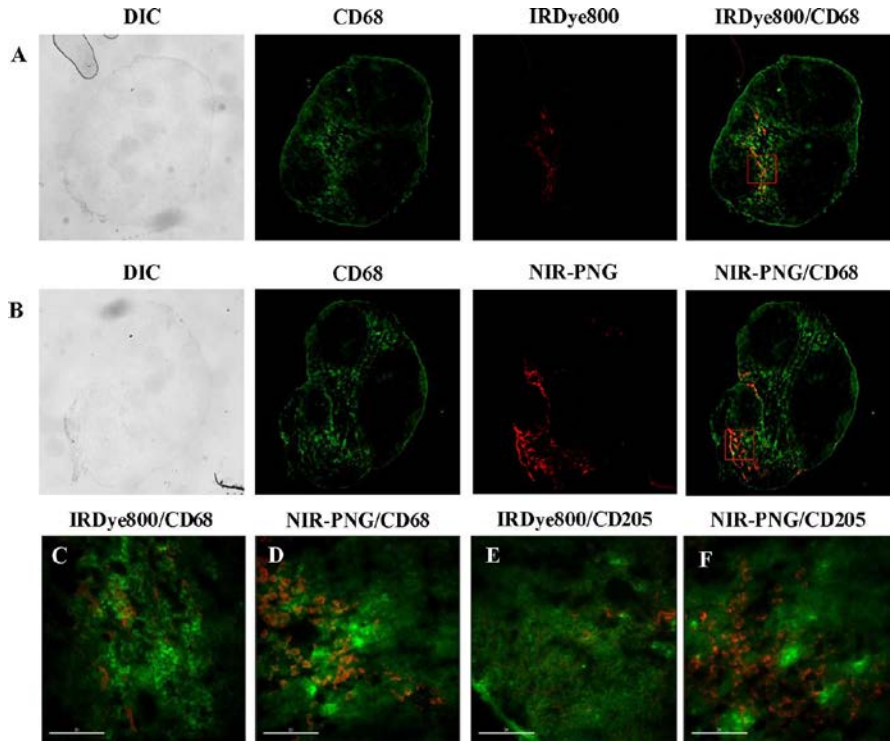

Figure 1-8. Immunohistofluorescence analysis of the sentinel lymph nodes. Images of the dissected sentinel nodes of a mouse injected with the IRDye800 dye (A, C, E) or NIR-PNG nanoprobes (B, D, F). The slides were stained with anti-CD68 (F4/80, macrophage, A-D) or anti-CD205 (DEC-205, dendritic cell, E, F). (C, D) Enlarged images of red squares. DIC, differential interference contrast; green, CD68 and CD205; red, IRDye800 and NIR-PNG (pseudocolor). Scale bars represent 90 μm.

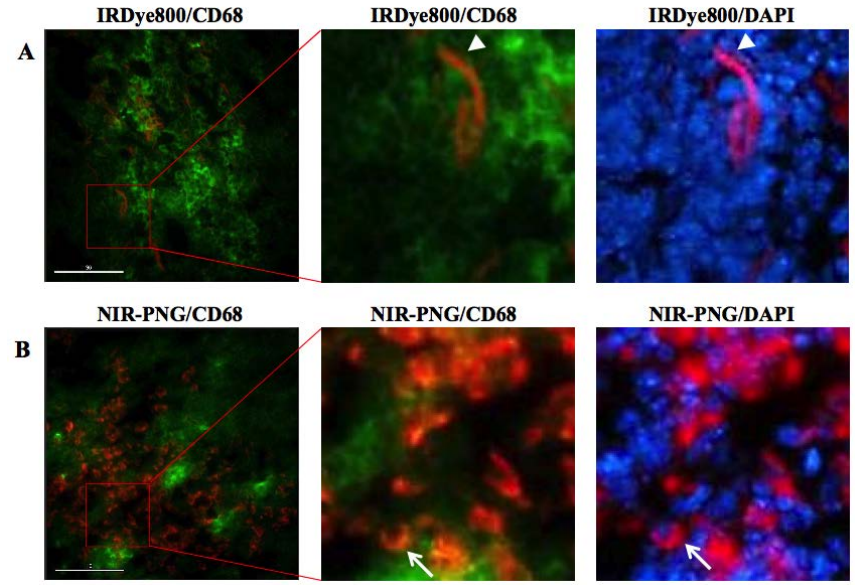

Figure 1-9. The enlarged images of Figure 1-8 C (A) and 1-8 D (B). arrowhead, NIR fluorescence signals outside of cells; arrow, NIR fluorescence signals inside of cells

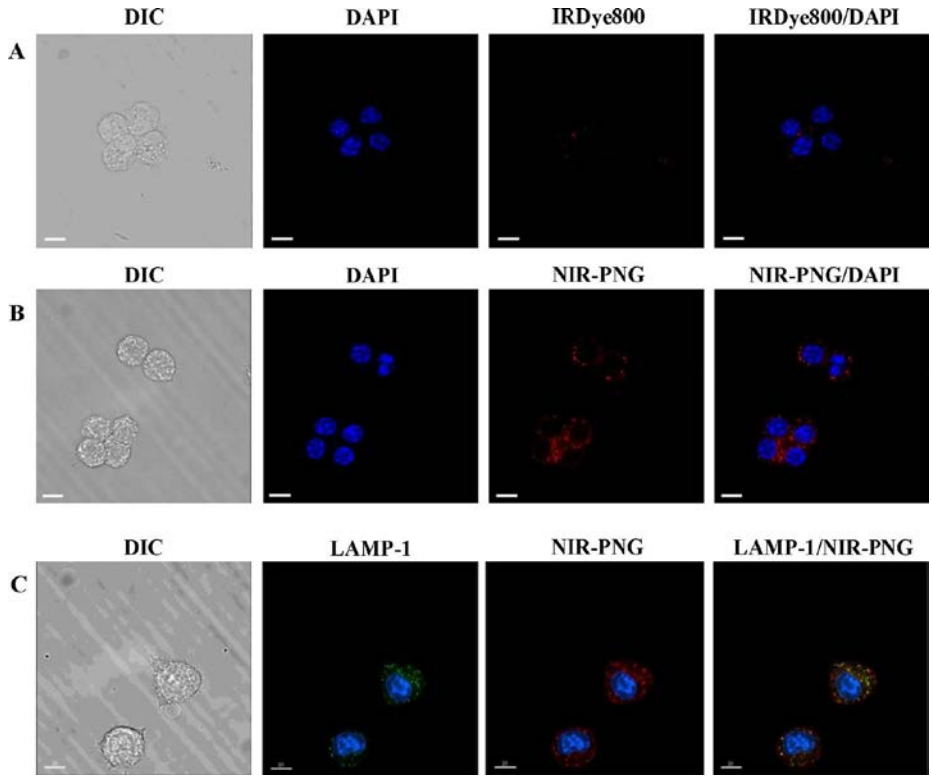

Figure 1-10. In vitro fluorescence images of NIR-PNG nanoprobes accumulated in the cell. Fluorescence microscopy images of DC2.4 cells treated with 2.5 μg/mL IRDye800 dye (A) and 0.1 mg/mL NIR-PNG nanoprobes (B). The NIR fluorescence images (red, pseudocolor) were obtained by using excitation (740/35 nm) and emission (780LP nm) filters. (C) DC2.4 cells, treated with NIR-PNG nanoprobes, were stained with FITC-conjugated LAMP-1 monoclonal antibody (green). Localization of lysosomes (green) and NIR-PNG nanoprobes (red, pseudocolor) was determined by fluorescence microscopy. Scale bars represent 10 μm; DIC, differential interference contrast.

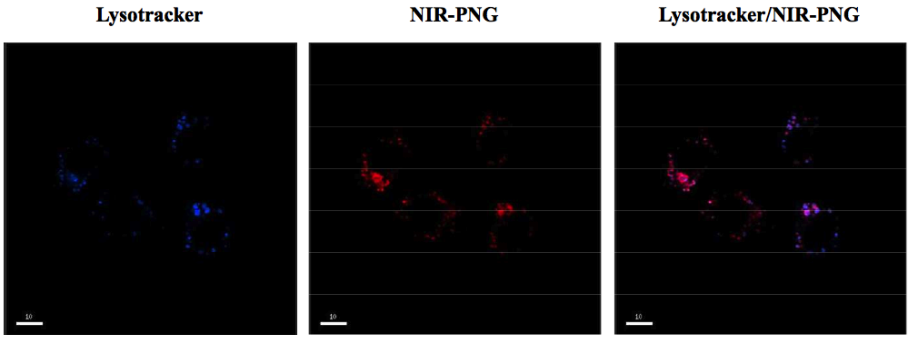

Figure 1-11. The localization of NIG-PNG nanoprobes within DC2.4 cells. The DC2.4 cells treated with 0.1 mg/ml NIR-PNG were stained with lysotracker blue for 30 min. Localization of lysosomes (blue) and NIR-PNG nanoprobes (red, pseudo-color) was determined by fluorescence microscopy. Scale bars represent 10 μm.

DISCUSSION

The NIR imaging technology has been proposed as a promising option for the sentinel lymph node biopsy due to several advantages. The visibility with very good sensitivity without a concern of biohazard is one of the distinguishing features that can replace the currently most sensitive sentinel node navigation technique using radioisotope, which require special detection device due to invisibility in naked eyes.

ICG, an organic NIR fluorophore, has been applied for NIR imaging of sentinel node mapping with excellent safety profile. However, its characteristics as a free particle result in too rapid and extensive dispersion, especially in gastric cancer[23], although it has been reported to be more sensitive than visual inspection methods or infrared imaging in gastric cancer.[32-34]

Out of three strategies previously described, ICG physically mixed with ɣ-PGA has been developed by collaborative researchers of this study. ɣ-PGA is produced by *Bacillus subtilis* during the fermentation process of soybeans and is being used in a broad range of biomedical, food, and cosmetics industries because of its minimal toxicity and immunogenicity.[35,36] ICG/ɣ-PGA complex was found to have and reported enhanced photostability and retention time in small animal experiments, which is probably caused by reduction of the aggregation of ICG and stabilization effect.[27]

In this study, we tried to optimize the concentration of ICG and develop a nanogel in an ideal size for sentinel node mapping. Although there is debates about the optimal size of the tracers, it is generally accepted that 10-50nm is ideal to move and stays in the sentinel nodes, because small particle in a small size can rapidly disperse to bloodstream or beyond the sentinel nodes, and

large particle does not easily move from the injection site to the lymph nodes.[28,30,31]

Although the inorganic fluorescent semiconductor nanocrystals (quantum dots) can be easily modifiable in size and have higher quantum yields, possible toxic core delayed clinical application to human. In contrast, pullulan is a a neutral linear polysaccharide produced from starch by *Aureobasidium pullulans* and has been used in biomedical field due to its water soluble, biodegradable, nontoxic, and nonimmunogenic properties, as well as its amenability to chemically modification.[31]

The signal of ICG *in vitro* was decreasing with a high concentration because of the tendency of aggregation of ICG and self-quenching effect. Although the signal was the brightest in 0.01mg/ml *in vitro*, the optimal concentration enough for the sentinel lymph node biopsy with minimal quenching effect seemed to be in between 0.1 and 1mg/ml *in vivo* experiment in pigs, probably due to dilution effect in the lymphatics.

The amount of injection also seemed to be sufficient with 0.1-0.2ml. Compared with conventional amount of ICG as a vital dye method, 5mg/ml in concentration and 0.5ml for each four injection, about 125 times less amount of ICG might be sufficient for NIR imaging system.[33,37,38] A smaller dosage could be advantageous in terms of less toxicity such as hypersensitivity reaction despite it is rare event for ICG.[39]

Like other vital dye including ICG, NIR-PNG followed general characteristic of dyes of which fluorescence intensity increases as the concentration of the dye increases; however, at a certain threshold concentration, the fluorescence intensity begins to decrease because the emitted photons are reabsorbed by other fluorescent dyes in the solution. [40] NIR-PNG nanoprobes did not influence the emission spectrum of IRDye800 and showed identical spectrum at room temperature. However, the

photostability of NIR-PNG was very much enhanced compared with that of IRDye800, which is advantageous in sentinel node mapping to provide prolonged and brighter signal in sentinel nodes. The brighter and prolonged signal seems to be mainly resulted from about 30nm's diameter, but the distribution patterns of NIR-PNG inside the lymph nodes implies the effect of phagocytosis can be additive reason. In the excised sentinel nodes, NIR-PNG was located in the subcapsular area where the macrophage and dendritic cells are located, however, most of IRDye800 was found outside those cells. Intracellular localization of NIR-PNG in DC2.4 cell lines indicated that internalized NIR-PNG nanoprobes preferentially localized in the lysosomal compartments of phagocytic cells. These results all explain why NIR-PNG nanoprobes could accumulate effectively in the lymph nodes.

For cytotoxicity studies, dendritic cell line (DC2.4) and an epithelial colorectal adenoma cell line (CT-26) were used because these dendritic cell lines were typical dendritic cells present in lymph nodes. No cytotoxic result and no effect on cytokine production supported the safety of NIR-PNG and applicability to clinical usage.

In conclusion, the optimal concentration of ICG to provide sufficient sensitivity with minimal quenching effect seemed to be between 0.1 and 1mg/ml in NIR imaging systems. The combination of NIR fluorescence dye and a nanosize polymer nanogel (PNG) dramatically improved the photostability and retention time of the NIR fluorophore in the sentinel lymph nodes in small animal models. These NIR tracers could be good options for sentinel lymph node mapping in further large animal model experiments and consequent clinical trials.

CHAPTER 2

Evaluation of large animal models and comparison of new tracers

INTRODUCTION

Because of the importance of lymph node metastasis and need for lymphadenetomy of various solid cancers, efforts to find regional lymph nodes around the primary cancer have made since decades of years ago in gastric cancer, melanoma, breast cancer, penile cancer, and so on. [41-44] The concept of sentinel lymph node navigation surgery, in which extensive lymphadenectomy of regional lymph node is not performed when the sentinel lymph node has no metastasis, have been applied to surgery since early 1990s, and now it became as effective treatment strategy as standard extensive surgery with less morbidities resulted from lymphadenectomy in breast cancer and malignant melanoma. [45-47] In gastric cancer, however, its efficacy is still under investigation due to the complex lymphatic structure around the stomach and significant false negativity.[4]

To test and apply the NIR tracers for various malignancies, an NIR fluorescence imaging system was designed for large animal models in cooperation with the research team of Chungnam national university. The NIR imaging facilities and some large some large animal models such as inguinal lymph node and small bowel model, which were used in previous studies, and breast cancer and gastric cancer models were evaluated for usefulness of assessment of NIR tracers and clinical applications. Especially, three tracers prepared by previous studies in chapter 1 was evaluated in gastric cancer model to determine whether they could overcome the drawback of ICG of dispersing quickly to multiple lymph nodes and whether they could be clinically applicable for gastric cancer using NIR imaging systems.

MATERIALS AND METHODS

1. NIR fluorescence imaging system

NIR imaging system consists of an excitation light source (780 nm, diode laser) and a cold charge-coupled device (CCD) camera (Orca ERG; Hamamatsu Photonics, Hamamatsu City, Japan) with an emission filter (845 nm band-pass filter), designed and built in Chungnam national university, Korea. (Figure 2-1)

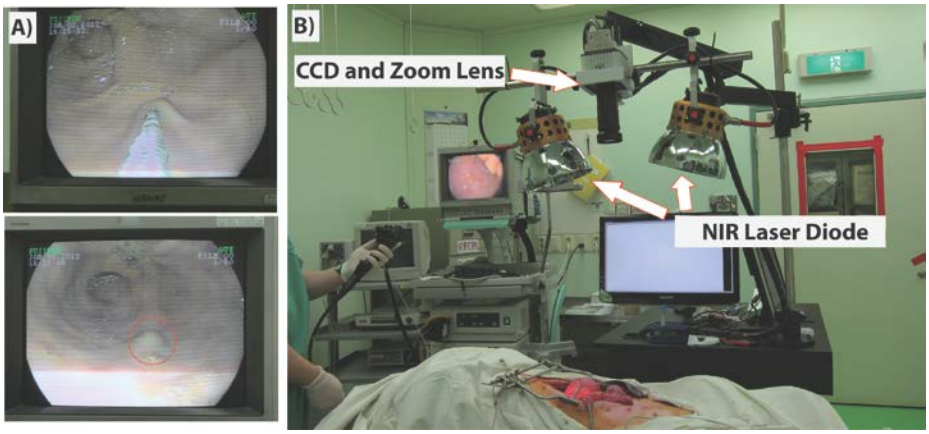

Figure 2-1. The setting of NIR fluorescence imaging facility and gastroscopy for large animal experiments
A) Gastroscopic injection of the tracer in the stomach, B) NIR fluorescence imaging system

2. Large animals

Female mongrel dogs (age ~50 weeks, weight ~30 kg) and female conventional pigs (age ~13 weeks, weight ~40 kg) were purchased and bred by Department of Experimental Animal Research, Clinical Research Institute, Seoul National University Hospital. All the protocols of animal experiment were approved by IACUC of Seoul National University Hospital. All the animals took more than 1 week of quarantine and adaptation period before experiments.

For the general anesthesia, 0.1ml/kg of zoletil® (Tiletamine 125mg, Zolazepam 125mg/ml, Virbac Korea), amd 0.1ml/kg of Rompun® (Xylazine

HCL 23.3mg/ml, Bayer Korea) was subcutaneously injected, followed by endotracheal intubation and ventilation of with 100% oxygen and maintainance with 1.5% to 2% sevoflurane or isofluran. For pigs, 0.25mg/kg of vecuronium bromide was additively administered subcutaneously. For the animals which were observed alive after the experiments, cefazolin was administered subcutaneously before the skin incision with a dosage of 25-30mg/kg, and meloxicam was administered with a dosage 0.4mg/kg subcutaneously before the recovery of anesthesia and with 1mg tablet per oral twice a day postoperatively.

3. Tracers

ICG, ICG/ ɣ -PGA complex, and NIR-PNG nanoprobe were prepared as described in chapter 1. The concentration of ICG was diluted as per the purpose of each experiment from 5mg/ml, which is the initial concentration of the commercial product and usually used in visual inspection method in sentinel node mapping. ɣ -PGA in 50kD was used and mixed with ICG in different concentration to prepare ICG/ ɣ -PGA complex. Methylene blue dye (1% concentration, Sigma-Aldrich, St. Louis, MO, USA) was used in the porcine inguinal node examination as a positive control for sentinel nodes.

4. Sentinel lymph node biopsy in breast cancer and melanoma model of large animal

To assess the quality of NIR camera system and to exam clinical applicability, tracers were injected around the most proximally located nipple and the thigh which simulate sentinel lymph node mapping for breast cancer and cutaneous malignancy of lower extremities, respectively, in both pig and dog models.

In the thigh of pigs, 0.2ml of ICG in different concentrations (0.01, 0.1, 0.2, 5mg/ml) or NIR-PNG was intradermally injected by 25 gauge needle, followed by injection of 0.2ml of methylene blue in case of NIR-PNG after identification of possible site of sentinel lymph node. In the thigh of dogs, different concentration (0.1, 0.5, 1, and 5mg/ml) and amount (0.2 or 0.5ml) of ICG and NIR-PNG was injected in the same method to assess the minimal requirement of ICG for the NIR imaging system.

For experiment of breast cancer model, ICG was injected adjacent to the most proximally located nipple in combination of different concentration and amount. (0.1, 0.5, 1, and 5mg/ml and 0.1, 0.2, and 0.5ml) After 10 minutes later, incision was made at the sites where the signal of lymphatic flows ended or the signal of lymph node was detected, then the sentinel lymph nodes were searched. NIR images were evaluated and compared with visual inspection of the color of ICG or methylene blue in terms of sensitivity and the location of sentinel lymph nodes

5. The small bowel model in pigs: a comparison of ICG and ICG/ɣ-PGA complex and histopathologic findings depending on three tracers

To compare the property of dispersion between ICG and ICG/ɣ-PGA complex, the mesenteric lymph nodes were exposed and injection sites of the small bowel were selected with enough distant between each other. ICG and ICG/ɣ-PGA complex were injected on the small bowel wall subserosally by 25 gauge needle in a combination of concentration (ICG 0.1 and 1 mg/ml, ɣ-PGA 0.1% and 1%). Time for travelling of tracers from the injection site to the first draining lymph node as well as time to the 2nd lymphatics or lymph nodes beyond the first lymph nodes was checked.

To find the duration of tracers and effects on histopathlogic the injection site and the lymph nodes, 0.1ml of ICG/ɣ-PGA complex (ICG 0.1mg/ml, ɣ-PGA 0.1%), and NIR-PNG nanoprobe were injected in the subserosal layer of the small bowel of a pig by 25 gauge needle. The injection site and the lymph node were removed 10 minutes after injection to be prepared for histopathologic examination. In other pigs, same tracers were injected in the same manner and NIR imaging was obtained 10 minutes later, then the injection sites and the lymph nodes were marked by 4-0 prolene suture. One pig was reexplored 2 days later for NIR imaging of remaining fluroscence signal of three tracers. The other pig was kept alive and reexplored 1 week later for NIR imaging and removal of the marked injection sites and lymph nodes. The tissues of the injection site and the lymph nodes were embedded in Tissue-Tek O.C.T. compound (SAKURA, Tokyo, Japan) and frozen in liquid nitrogen. Cryosections (8 mm) were cut by a Tissue-Tek Cryo3 Microtome/ Cryostat (SAKURA) and transferred to glass slides. The sections were fixed with cold acetone for 5 min and were dried and frozen at -20°C. The slides were washed in PBS and blocked with PBS containing 1% BSA for 1 h at room temperature. After an additional series of washes, the slides were treated with DAPI in PBS for 10 min or stained by hematoxylin and eosin (H&E). After the final washing, the slides were mounted in 50% glycerol (in PBS) and examined by a fluorescence microscope (Olympus IX71, Olympus Optical, Tokyo, Japan) and a DeltaVision PD Restoration Microscope System (Applied Precision Technologies, Issaquah, WA, USA).

H&E stained slides were reviewed by an experienced pathologist in Seoul National University Hospital

6. Sentinel lymph node biopsy in the stomach of dogs and pigs

6.1. The canine stomach model

To compare the properties of tracers in the lymphatic system around the stomach, 0.1ml of ICG (0.1 mg/ml), ICG/ɣ-PGA complex (ICG 0.1mg/ml, ɣ-PGA 0.1%), and NIR-PNG nanoprobe were injected in the subserosal layer at the greater curvature side of the lower body of the stomach using 25 gauge needle. The pattern and time of the tracers to travel to the first lymph node and the next lymph nodes were observed and compared. The injection site and the first lymph node were marked with metal clips and the dogs were recovered from the anesthesia and kept alive, and the marked injection site and the lymph nodes were re-explored 1 week later. In one dog, an endoscopic NIR-PNG injection was followed by an injection of 0.5 ml of 0.5 mg/ml of ICG in the same manner as in the experiments in pigs described in the next paragraph.

6.2. The porcine stomach model

Gastroscope (EG-450WR5 with E400 system, Fujinon, Tokyo, Japan) was inserted through an overtube into the stomach, and 0.2ml of ICG (0.1 mg/ml), ICG/ɣ-PGA complex (ICG 0.1mg/ml, ɣ-PGA 0.1%), and NIR-PNG nanoprobe were injected in the submucosal layer at the greater curvature side of the lower body of the stomach using 23 gauge endoscopic injection needle (NM-400U-0423, Olympus, Aomori, Japan). After about 30 minutes of observation with the NIR camera system, 0.5ml of 5mg/ml ICG was injected at the same site to compare the NIR images and the visual inspection method in terms of sensitivity and patterns of distribution of the tracers.

RESULTS

1. Sentinel lymph node biopsy in breast cancer and melanoma model of large animal

Inguinal lymph node biopsy of pigs

Injection of ICG and tracers in the thigh of pigs revealed very good sensitivity of NIR imaging system. (Figure 2-2) Compared with methylene blue and ICG in a concentration of 5mg/ml, which is usually used in the visual inspection method in the sentinel lymph node biopsy, NIR images of ICG, NIR-PNG, and ICG/PGA complex were better to clearly show not only the sentinel lymph nodes but also the dermal lymphatic flow between the injection site and the lymph nodes. The locations of the sentinel lymph node which methylene blue indicates were identical to those indicated by ICG or NIR-PNG, and the bright signal of the sentinel lymph nodes by the NIR system was better to be identified and larger than vital dyes. The fluorescence signal of the lymph node also showed deep penetration enough to identify the location of the lymph node through the skin around the area where the signals of dermal lymphatic flows end. Sentinel lymph node could be found by 0.05mg of ICG, but 0.005mg of ICG was not enough to show lymphatic flows or lymph nodes even though the injection site was brightly shown.

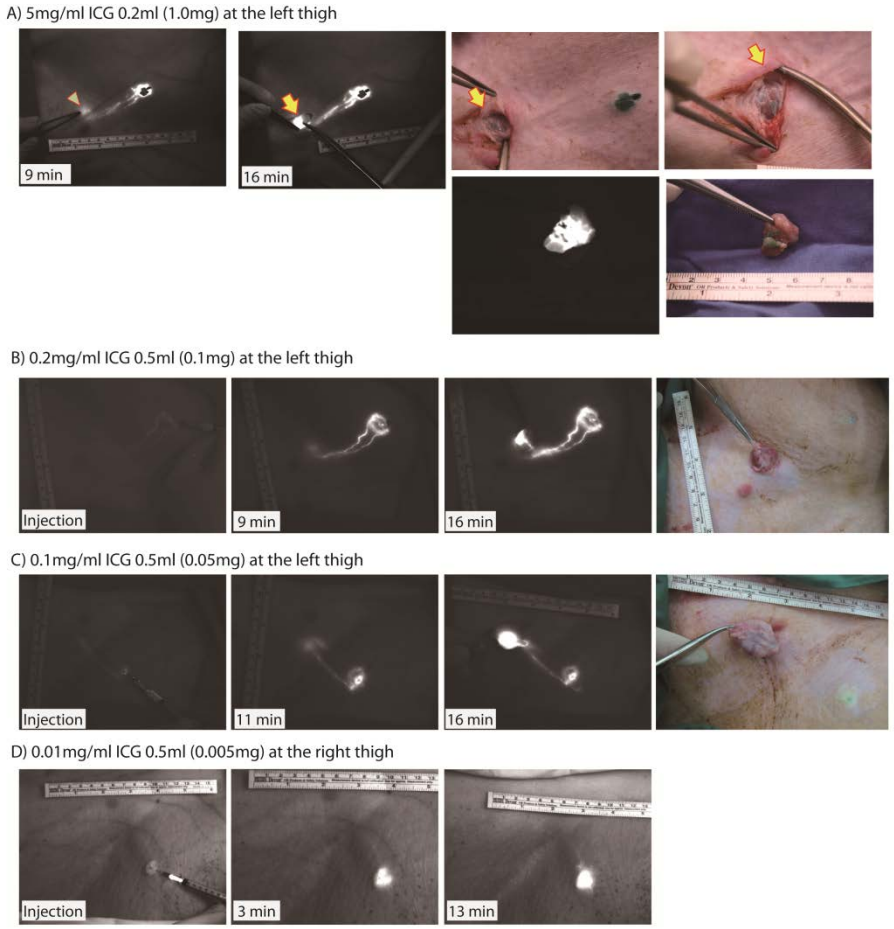

(continued in the next page)

Figure 2-2. Sentinel lymph node biopsy in the inguinal area of pigs using ICG, NIR-PNG followed by methylene blue, and ICG/PGA complex. NIR images were highly visible compared with ICG or methylene blue as vital dyes. The lymph nodes identified by NIR images were identical to those located by methylene blue. A-D) Injection of different amount of ICG at the thigh, E, and F) Injection of 0.2ml of NIR-PNG followed by injection of 0.2ml of methylene blue in different pigs. Concomitant injection of methylene blue interfered the NIR signal in the lymphatics. G) Injection of ICG/PGA complex. Arrowhead: the signal from the lymph node through the skin, Arrow: The sentinel lymph nodes

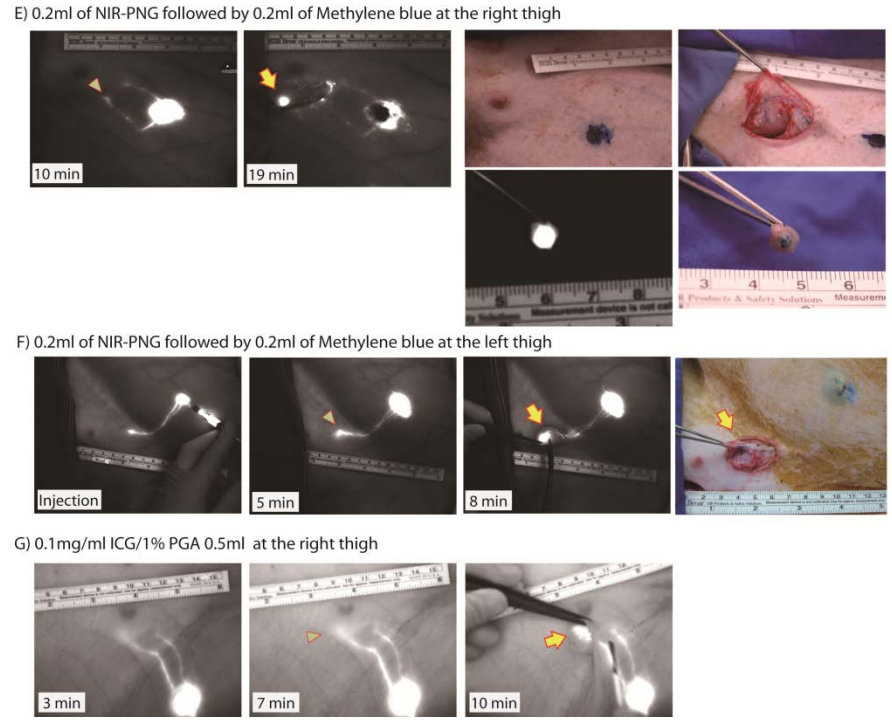

Inguinal lymph node biopsy of dogs

In experiments of canine model which was purposed to assess sensitivity of NIR system, NIR image was sensitive to identify the sentinel lymph node with ICG in a concentration of 0.5mg/ml which is 10 times diluted from the concentration used for visual inspection. Sentinel lymph node could be found by 0.2mg of ICG, but 0.02mg of ICG was not enough to show lymphatic flows or lymph nodes even though the injection site was brightly shown. (Figure 2-3)

Sentinel lymph node biopsy of the breast in pigs

In experiments of porcine breast cancer model where the tracers were injected around the most proximal nipple, the lymphatic flows travelled not to the axillary area but to the deep cervical area where it was difficult to find the sentinel lymph nodes, (Figure 2-4. A, B, and D) and even to the inguinal

lymph nodes along more than 45cm's distance of dermal lymphatic flow in one case. (Figure 2-4 C) When comparing 0.1ml of 5mg/ml ICG and 0.5ml of 1mg/ml ICG, larger amount of ICG in a lower concentration seemed to be better to track the lymphatic flows and lymph nodes in the same amount of ICG. The case in which the tracer moved to the inguinal lymph node showed the importance of individual variation of lymphatic flows and the need of sentinel lymph node navigation, as well as the applicability of NIR camera system in cutaneous malignancies located in the extremities which lymphatic flows travel a long distance.

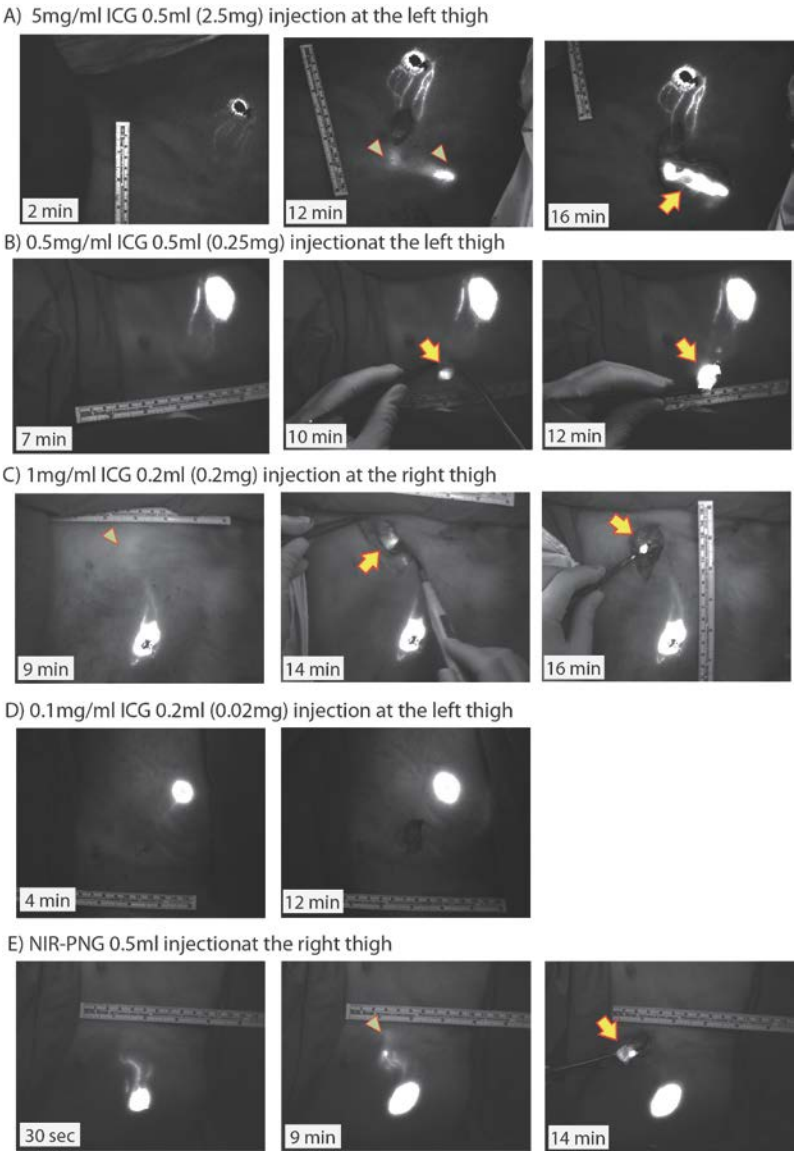

Figure 2-3. Sentinel lymph node biopsy in the inguinal area of dogs using ICG and NIR-PNG. A,B,C, and D) Injection of ICG in various dosage at the thigh of different dogs. ICG in 0.02mg was not sufficient to identify lymphatic flows. E) Injection of 0.2ml of NIR-PNG at the right thigh of a dog. Arrowhead: the signal from the lymph node through the skin, Arrow: The sentinel lymph nodes

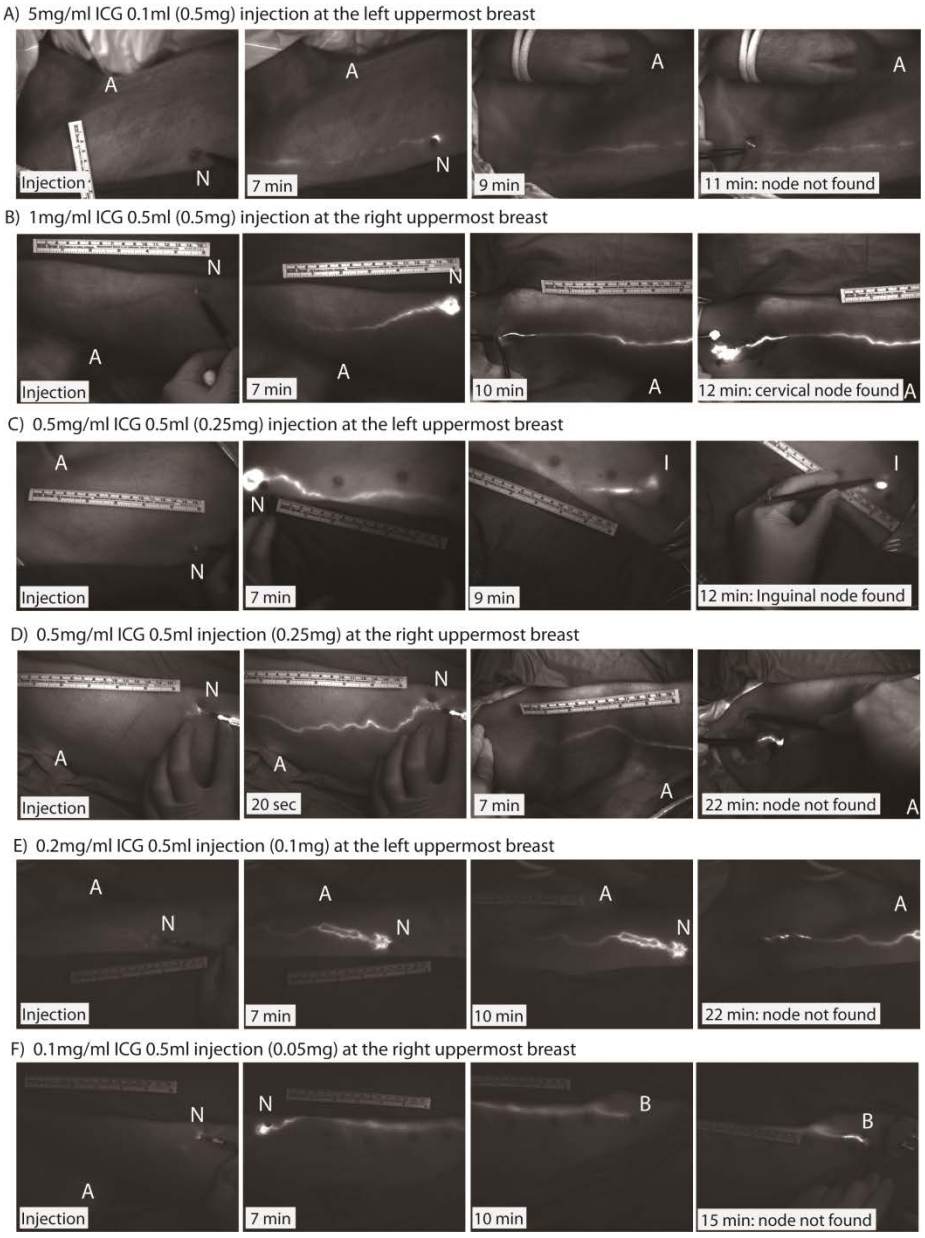

Figure 2-4. Injection of ICG in different amount at the uppermost nipple in pigs. A,D, and E) The NIR signal moved to cervical area, but only lymphatic vessel was found. B) The NIR signal moved to cervical lymph node. C and F) The NIR signal moved down to the inguinal lymph node and the breast tissue. A: Axillary area, B: Breast, N:The most proximal nipple, I: Inguinal lymph node

Sentinel lymph node biopsy of the breast in dogs

NIR camera system clearly showed the lymphatic flows in the dermal layer and large conglomerated axillary lymph nodes through the incision at the end of the signal of dermal lymphatics 10 minutes after the injection. (Figure 2-5) Sentinel lymph node could be found with 0.1mg or much amount of ICG, but no lymph node was identified with 0.05mg of ICG.

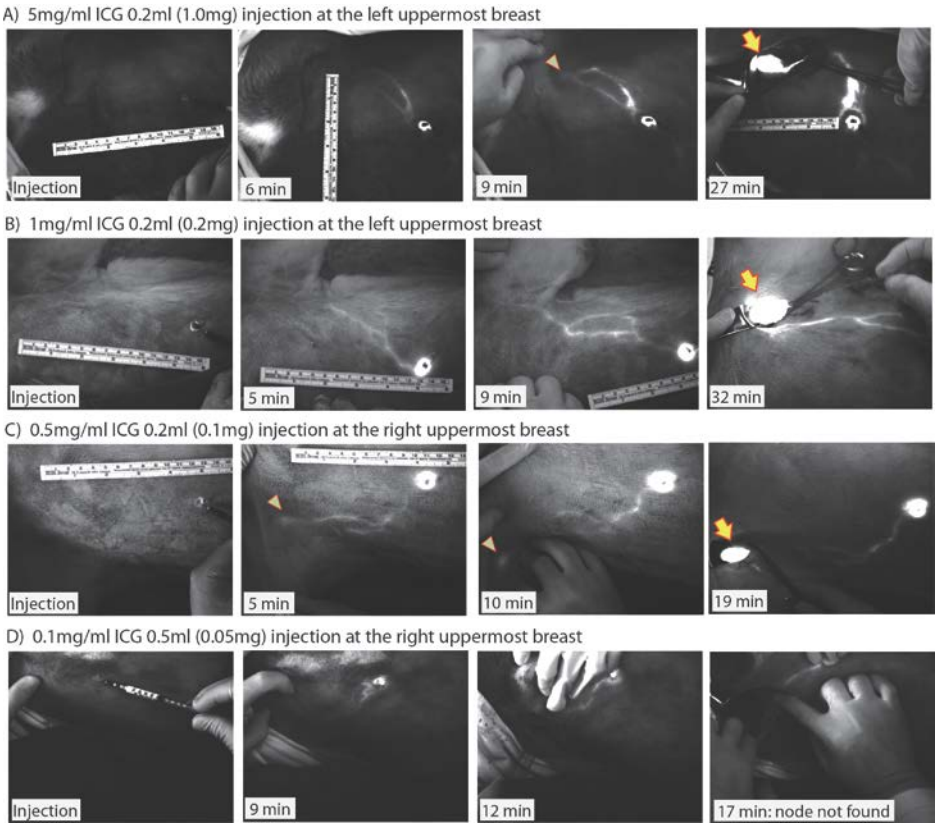

Figure 2-5. Injection of ICG around the uppermost nipple in dogs. A, B, and C) Injection of different dosages of ICG. The sentinel lymph nodes were identified by chasing the NIR signal in the axillary area. D) 0.05mg of ICG was not sufficient to identify the sentinel lymph node. Arrowhead: the signal from the lymph node through the skin, Arrow: The sentinel lymph nodes

The breast cancer in inguinal lymph node model in dogs and pigs showed high sensitivity of NIR imaging system with ICG in lower concentration than that used for visual inspection or NIR-PNG. However, the properties of

passing beyond the first lymph nodes of tracers could not be evaluated in these models because the lymph nodes were large and deep-seated.

The small bowel model in pigs and the comparison of ICG and ICG/ɣ-PGA complex

All the injection of tracers with a combination of concentration of ICG (0.1 and 1mg/ml) and ɣ-PGA (0.1 and 1%) resulted in bright signals in the lymphatic vessels and the first draining lymph nodes within a few minutes. (Figure 2-6) Signals in the lymphatic flows beyond the first lymph node were frequently observed and it seemed to be not related with the component or concentration of the tracers. The 2nd lymph nodes were not easily identified, and the most of the lymphatic flows moved into the systemic lymphatic system which is too deep to be explored.

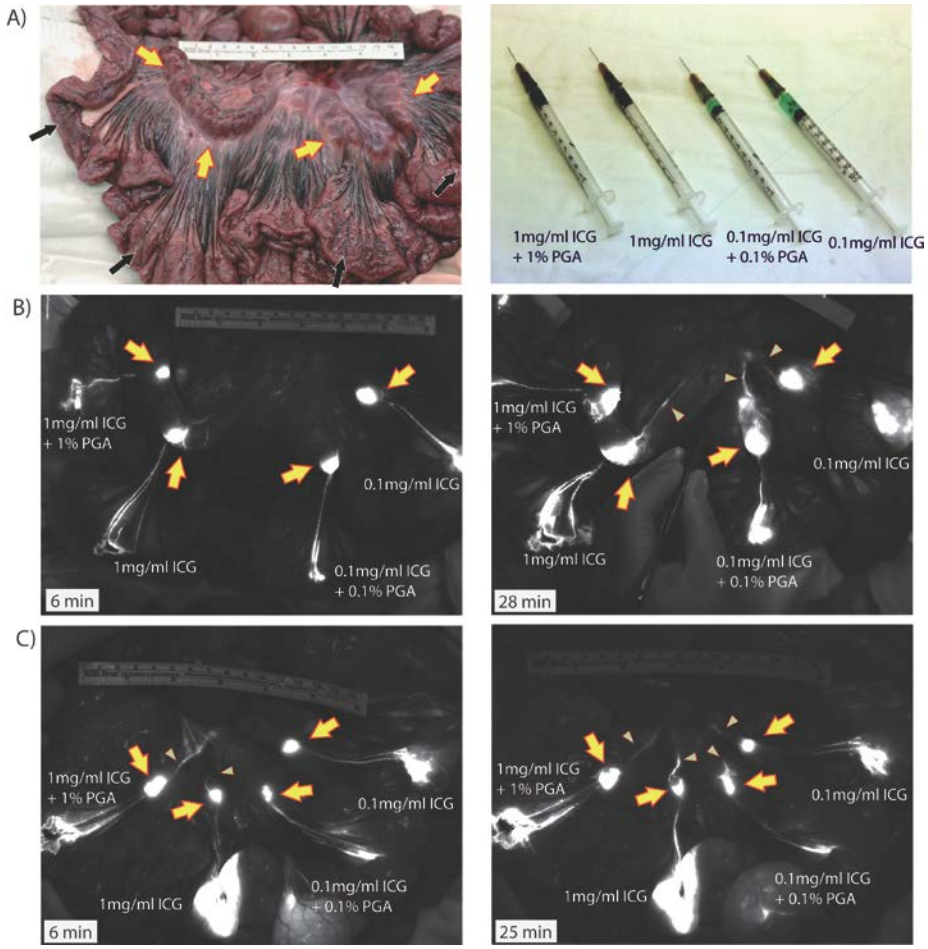

Figure 2-6. NIR imaging of lymphatic flows in the small bowel and mesenteric lymph nodes of pigs. A) The sites of injection and the mesenteric lymph nodes. B and C) The first draining lymph nodes and the lymphatic flows beyond it in two pigs. The pattern was similar regardless of the tracers. Black arrow: injection site, Yellow arrow: the first draining lymph node, Arrowhead: lymphatic beyond the first lymph node

Sentinel lymph node mapping in the canine stomach model

ICG and ICG/ɣ-PGA complex rapidly dispersed into multiple directions immediately after the injection; proximal and distal direction along the greater curvature in case of ICG, and the lesser and greater curvature side in case of ICG/ɣ-PGA complex. (Figure 2-7) The infrapyloric lymph node (sentinel node) was identified bright within several minutes, and the suprapancreatic lymph nodes with a bright signal were also found beyond the sentinel node. In case of NIR-PNG, no further lymph node was found beyond the sentinel

lymph node in the infrapyloric area until one hour after the injection. The shape of the injection site of ICG and ICG/ɣ-PGA complex was sprawling out with spikes, however, the shape of NIR-PNG at the injection site was spherical.

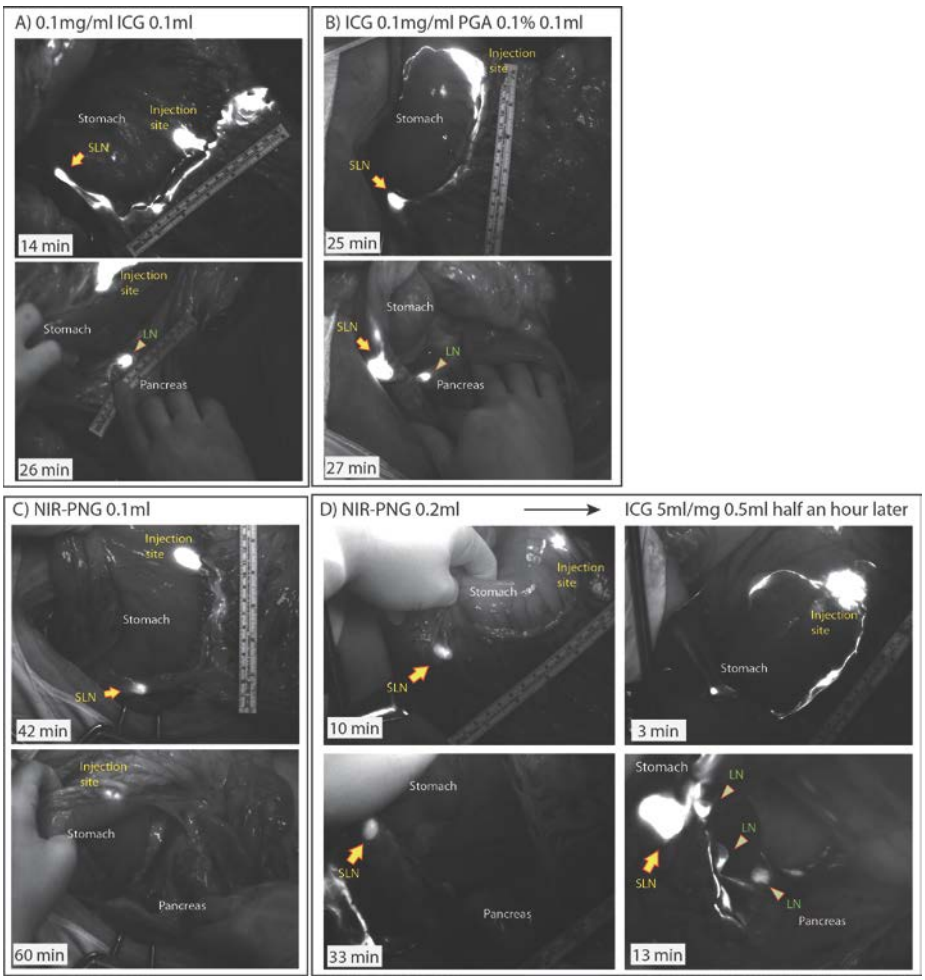

Figure 2-7. Sentinel lymph node navigation using 0.1ml of A) ICG, B) ICG/ɣ-PGA, and C) NIR-PNG injected in the canine stomach. The lymph nodes after sentinel nodes were identified in the suprapancreatic area in case of ICG and ICG/ɣ-PGA, however, no lymph node beyond sentinel node was found in case of NIR-PNG during about 1 hour. D) Endoscopic injection of 0.2ml of NIR-PNG also revealed no lymph node after sentinel node, and multiple nodes were identified after injection of 0.5ml of 0.5mg/ml ICG at the same site.

Duration of tracers and effect of tracers to histopathologic features in the injection sites and lymph nodes

Reexploration of the pig 2 days after the injection of tracers into the small bowel showed that the fluorescence signal of all three tracers remained at both the injection site and the lymph nodes. However, reexploration of the pig 1 week later showed that very small amout of ICG and ICG/ɣ-PGA complex remained, however, the signal of NIR-PNG was strong,

Likewise, in the re-exploring of the stomach of dogs 1 week after the injetion, no fluorescence remained at both the injection site and the lymph nodes for ICG and ICG/ɣ-PGA complex, however, the signal of NIR-PNG could be found in both sites. (Figure 2-8)

Histopathologic review of H&E stained slides, which is made by the injection site and the lymph node of the small bowel of pigs, showed that the numbers of follicles in the lymph node increased moderately with ICG/ ɣ-PGA complex and highly with NIR-PNG, compared by that with ICG in the lymph nodes removed 1 week after the injection, which seems to be resulted by reaction to remaining tracers. Otherwise, there was no significant difference in the finding of lymph nodes removed 10 minutes after injection or the finding of injection sites of both injection day and 1 week later. (Figure 2-9)

In the fluoresences microscopic images of the injection site and the lymph nodes of pigs, which were removed 1 week later (tissue of Figure 2-8 E), showed strong fluorescence signal in both the injection site and the lymph node in NIR-PNG, but only scanty fluorescence signal were identified in ICG or ICG/ ɣ-PGA complex-injected small bowel or lymph nodes. Some of red fluorescence signal of IRDye800 surrounded the nucleus in the shape of cells, implying the particle might be placed into the cytoplasm by phagocytosis. (Figure 2-10, 11)

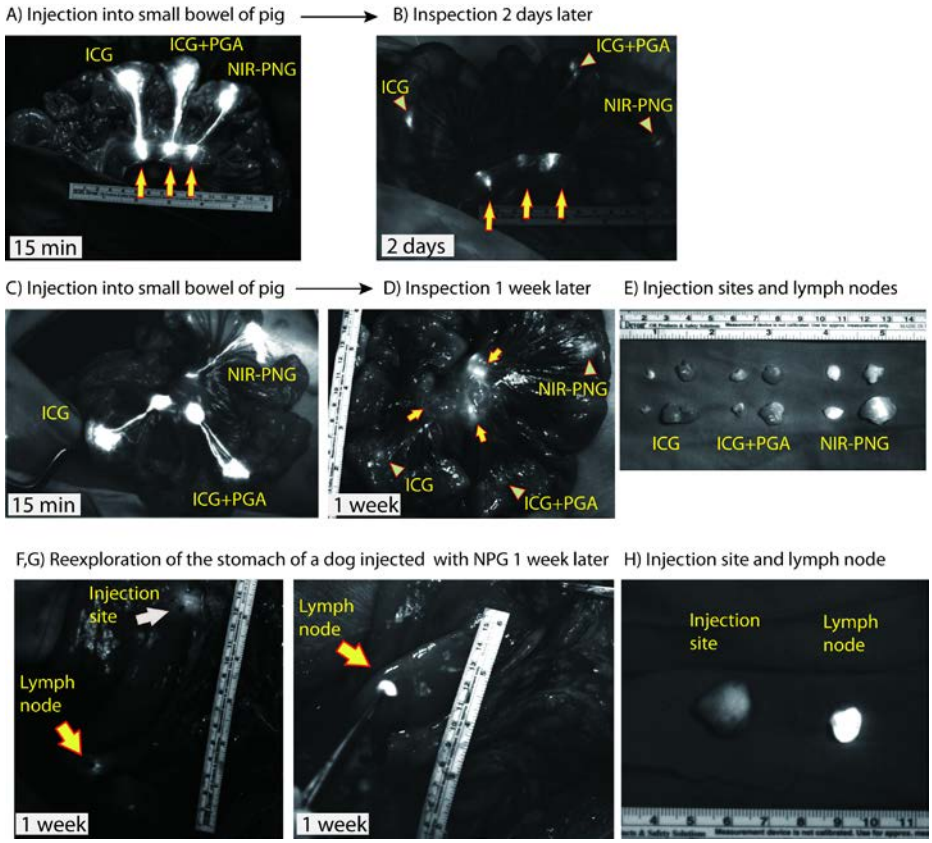

Figure 2-8. Delayed images of tracers. A and B) Fluorescence signals at injection sites and lymph nodes of all tracers in the porcine small bowel were identified 2 days later. C,D,E) One week after the injection of tracers in the porcine small bowel, bright NIR signal of NIR-PNG remained in the injection and the lymph node, but small amount of NIR signal of ICG and ICG/γ-PGA remained. F,G,H) The signals in canine stomach were identified in case of NIR-PNG 1 week after the injection, but no signal was found in the dogs injected by ICG and ICG/γ-PGA. Arrow: lymph node, Arrowhead: injection site

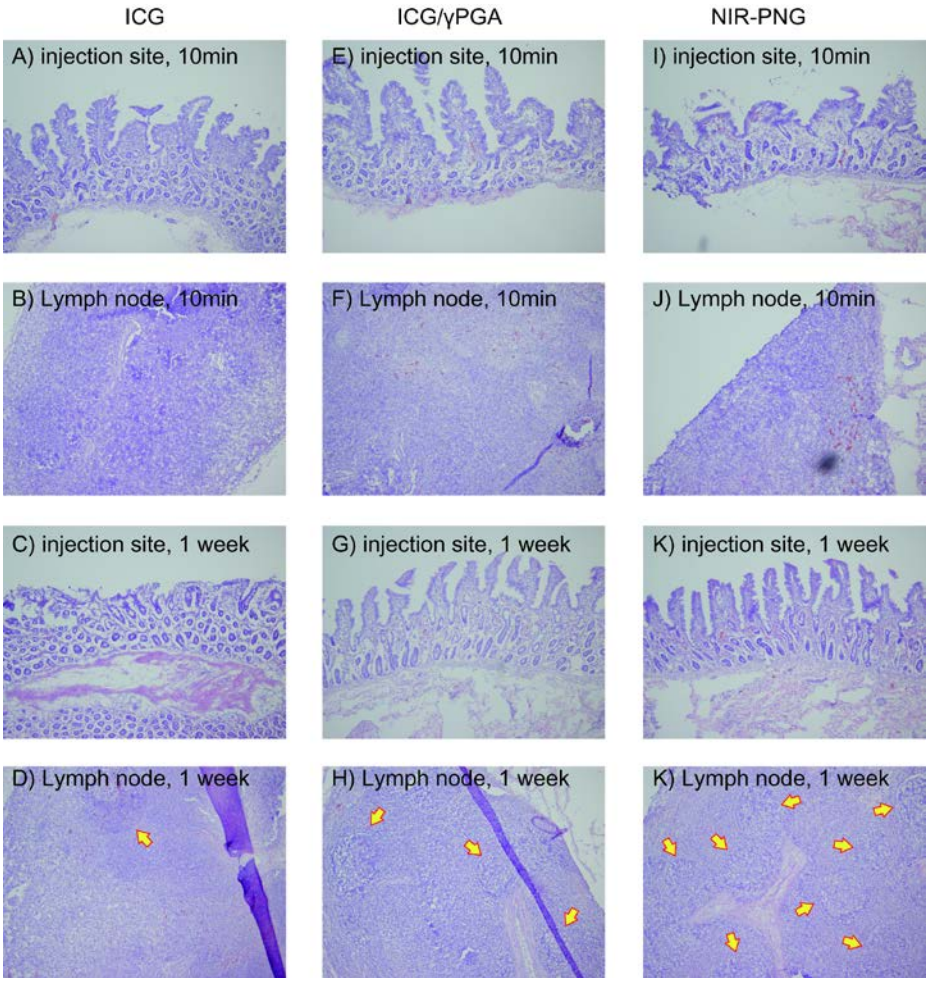

Figure 2-9 H&E stain of the injection sites and the lymph nodes removed 10 minutes and 1 week after injection of ICG (A-D), ICG/γ-PGA (E-H), and NIR-PNG (I-K). (x200) The lymph node 1week after injection showed moderate follicular hyperplasia in ICG/ γ-PGA (H) and significant follicular hyperplasia in NIR-PNG (K) compared with normal appearance in ICG (D). arrow: follicular hyperplasia

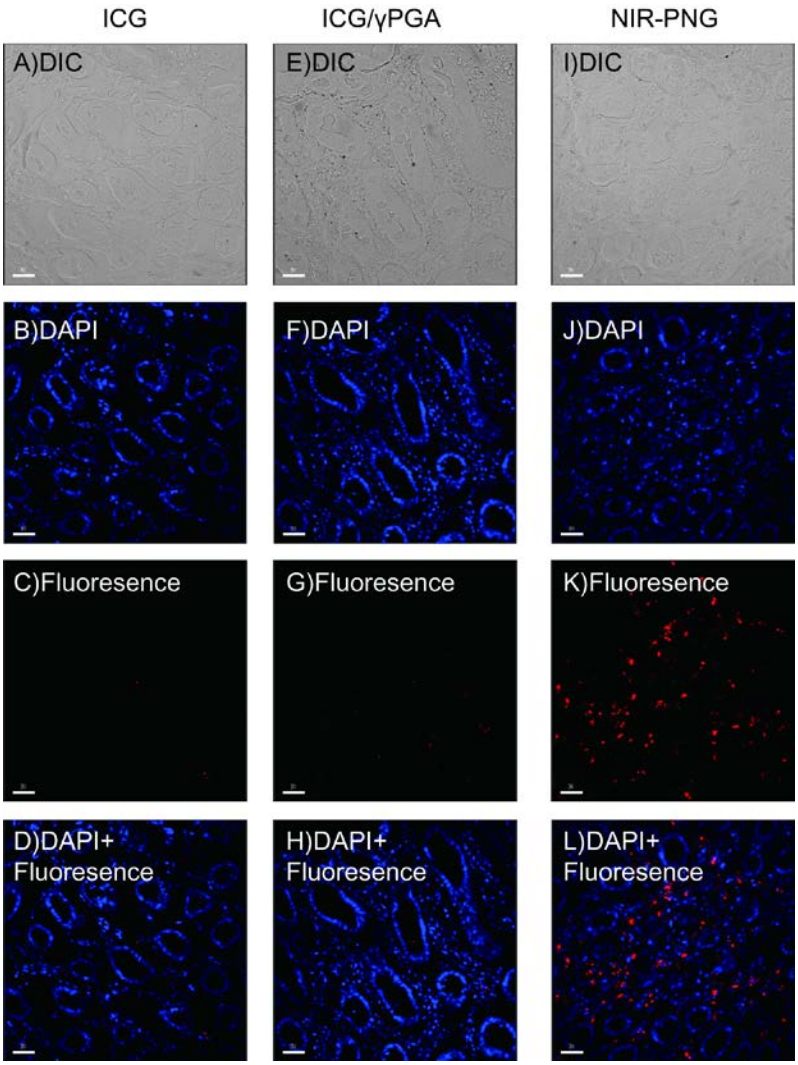

Figure 2-10 Fluorescence microscopic images of the injection site of the small bowel taken 1 week after injection. (x100) The fluorescent signal was barely seen in ICG (C,D) or ICG/ ɣ-PGA(G,H), but abundant in NIR-PNG (K,L)

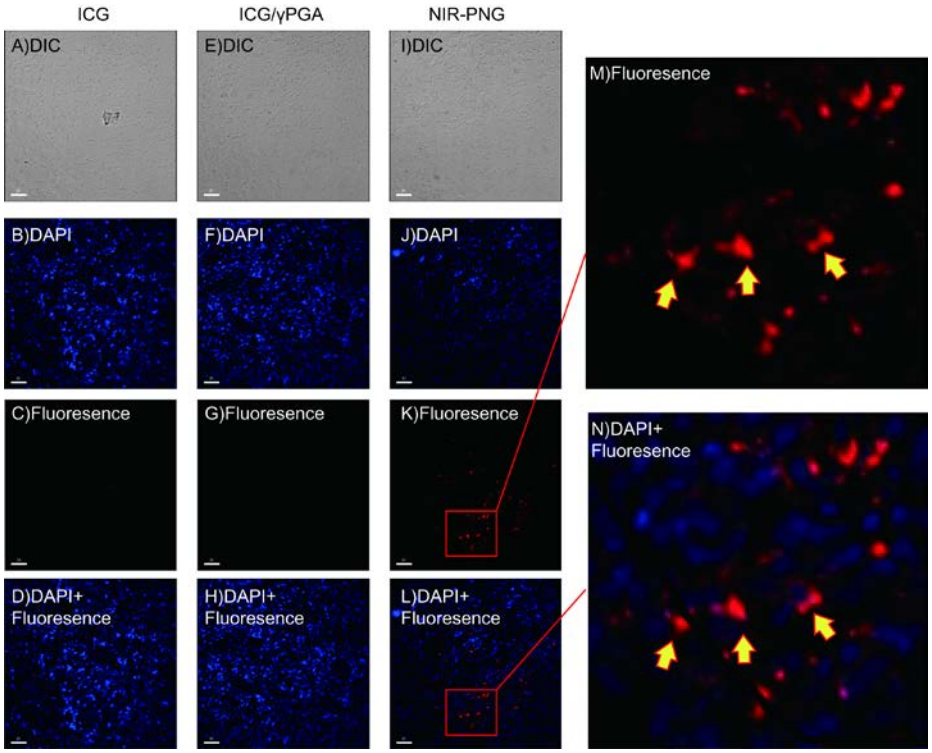

Figure 2-11 Fluorescence microscopic images of the lymph node of the small bowel taken 1 week after injection. (x100) The fluorescent signal was barely seen in ICG (C,D) or ICG/ γ-PGA(G,H), but abundant in NIR-PNG (K,L). Magnified view (M,N) showed that the tracer signal (arrow) surrounded the nucleus in the shape of cell, which implies phagocytosis of tracer into the cytoplasm.

Sentinel lymph node mapping in the porcine stomach model

Similar to experiments in canine models, ICG and ICG/ɣ-PGA complex spread along the both lesser and greater curvature side of the stomach immediately after the endoscopic submucosal injection, and showed multiple lymph nodes. (Figure 2-12 A,B,C and D) On the contrary, NIR-PNG identified only one lymph node and did not moved beyond during more than 30minues of observation. (Figure 2-12 E and F) The shape of injection site was centrifugal spreading pattern with spikes in ICG and ICG/ɣ-PGA, but spherical shape in NIR-PNG.

Compared with the green color observed by naked eyes after an injection of ICG with a concentration (5mg/ml) used for visual inspection which was difficult to be differentiated from venous vessels, NIR image was more sensitive and discernible from other tissues. NIR images of 5mg/ml of ICG revealed more lymph nodes beyond the first lymph node where NIR-PNG indicated.

The results in dogs and pigs were summarized in table 1.

Figure 2-12. Sentinel lymph node biopsy by endoscopic submucosal injection in gastric cancer model of pigs. A and B) ICG, C and D) ICG/ɣ-PGA, E and F) NIR-PNG in 2 pigs. Thirty minutes after the injection of tracers, 0.5ml of 5mg/ml ICG was injected at the same injection site, and the same area was observed by visual inspection and NIR imaging. Arrow: The first draining lymph node. Arrowhead: lymph node or lymphatic vessels beyond the first lymph node or identified additively after injection of 5mg/ml ICG

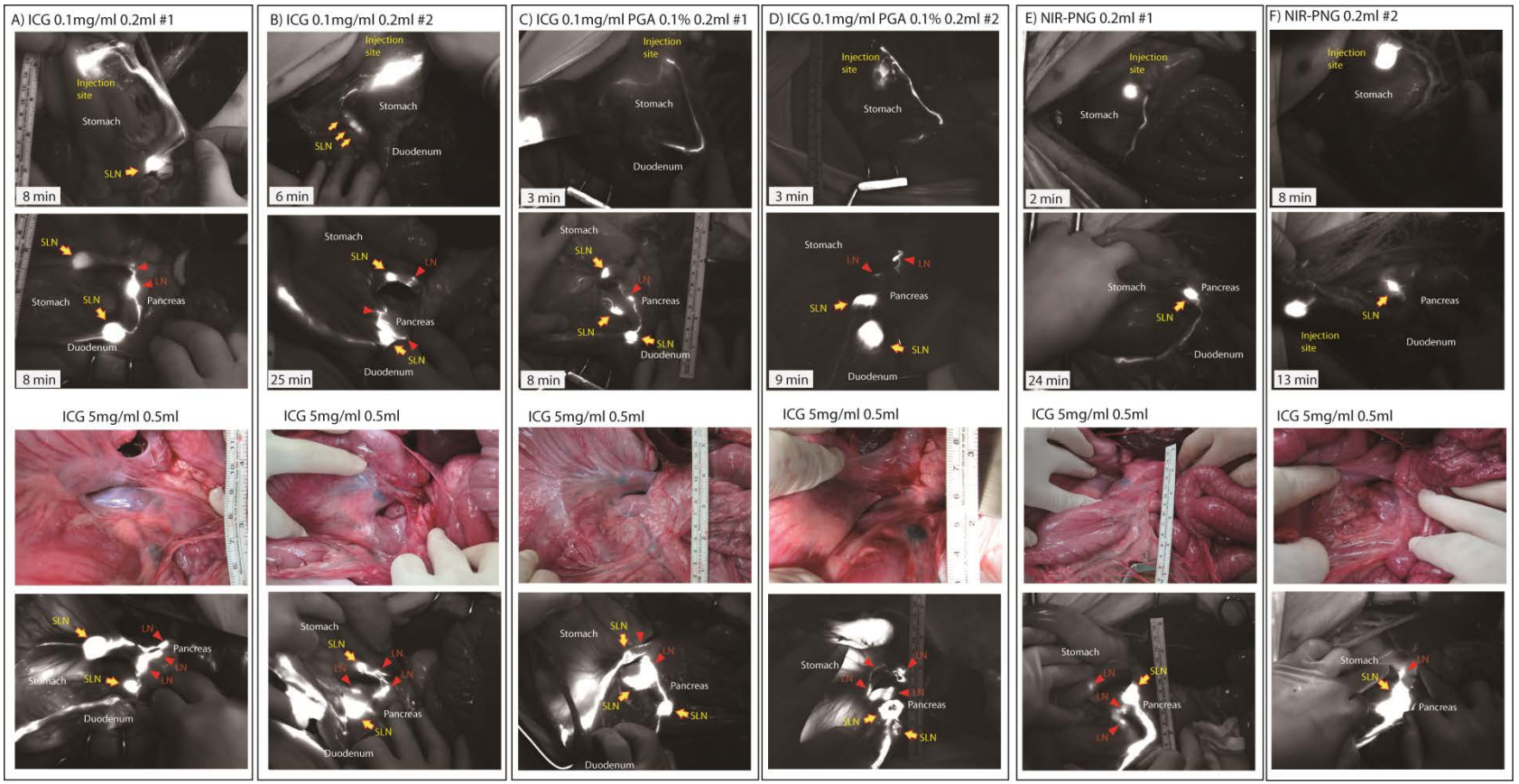
A) ICG 0.1mg/ml 0.2ml #1
Injection site
Stomach
SLN
8 min
SLN
LN
Stomach
SLN
Pancreas
Duodenum
8 min
ICG 5mg/ml 0.5ml
SLN
LN
Pancreas
Stomach
SLN
LN
LN
Duodenum
B) ICG 0.1mg/ml 0.2ml #2
Injection site
Stomach
SLN
Duodenum
6 min
Stomach
SLN
LN
Pancreas
SLN
Duodenum
25 min
ICG 5mg/ml 0.5ml
Stomach
SLN
LN
LN
LN
Pancreas
SLN
Duodenum
C) ICG 0.1mg/ml PGA 0.1% 0.2ml #1
Injection site
Stomach
Duodenum
3 min
Stomach
SLN
LN
Pancreas
SLN
SLN
Duodenum
8 min
ICG 5mg/ml 0.5ml
Stomach
SLN
LN
Pancreas
SLN
SLN
Duodenum
D) ICG 0.1mg/ml PGA 0.1% 0.2ml #2
Injection site
Stomach
3 min
Stomach
LN
LN
SLN
Pancreas
SLN
Duodenum
9 min
ICG 5mg/ml 0.5ml
Stomach
LN
LN
LN
LN
Pancreas
SLN
SLN
E) NIR-PNG 0.2ml #1
Injection site
Stomach
2 min
Stomach
Pancreas
SLN
Duodenum
24 min
ICG 5mg/ml 0.5ml
Stomach
LN
SLN
LN
Pancreas
LN
F) NIR-PNG 0.2ml #2
Injection site
Stomach
8 min
Pancreas
SLN
Injection site
Duodenum
13 min
ICG 5mg/ml 0.5ml
Stomach
LN
SLN
Pancreas

Serial number	Tracers	Injection Route	Body weight	Size of injection site	Shape of injection site	Direc-tion	1st LN detection time	1st LN number	Lymp-hatics after 1st LN	LNs after 1st LN	Obser-vation time	Additional injection	Additional LN found
Dog													
1	ICG	Subserosa	29kg	2.8x1.2cm	circular	1 (GC)	12min	2	1	1	60min		
2	ICG+PGA	Subserosa	29.5kg	3.1x1.5cm	Triangular	2 (LC, GC)	10min	3	1	1	75min		
3	PNG	Subserosa	32.5kg	2.0x1.2cm	circular	1 (GC)	22min	**1**	**0**	**0**	75min		
4	PNG	submucosa	30kg	1.9x1.4cm	circular	1 (GC)	9min	**1**	**0**	**0**	35min	ICG5mg/ml	4
Pig													
1	ICG	submucosa	34kg	2.3x1.5cm	Circular with spikes	2 (GC)	2min	2	1	1	30min	ICG 5mg/ml	2
2	ICG	submucosa	35kg	3.9x1.4cm	Out-spreading	2 (LC, GC)	2min	4	2	1	30min	ICG 5mg/ml	2
3	ICG+PGA	submucosa	39.5kg	1.7x1.5cm	circular	2 (LC, GC)	3min	3	3	2	30min	ICG 5mg/ml	2
4	ICG+PGA	submucosa	33kg	2.0x1.8cm	circular	1 (GC	2min	2	2	2	30min	ICG 5mg/ml	2
5	PNG	submucosa	42kg	1.4x1.4cm	circular	1 (GC)	3min	**1**	**0**	**0**	30min	ICG 5mg/ml	3
6	PNG	submucosa	37.5kg	1.9x1.7cm	circular	1 (GC)	5min	**1**	**0**	**0**	30min	ICG 5mg/ml	2

Table 1. Summary of the results of stomach model in dogs and pigs. NIR-PNG showed relatively smaller size of injection site signal, fewer numbers in flow direction and sentinel lymph nodes with no lymph node identified after the sentinel lymph node.
LN: lymph node, LC: Lesser curvature, GC: greater curvature

DISCUSSION

In this study, we could identify high visual sensitivity and feasibility of clinical application of our own-made NIR imaging system using ICG and IRdye-based tracers in the large animal models simulating breast cancer and cutaneous malignancy, for which diseases the NIR imaging system has been already applied for human trials. [12,13,48,49] The NIR images were highly sensitive to show not only the lymph nodes but also the cutaneous lymphatic flows which cannot be identified as clear by vital dyes, and not easily detected by radioisotope system. The breast cancer model in pig was found to be not a good model for sentinel node mapping, because of unpredictable lymphatic flows into other than axillary lymph nodes and difficulties to find the deep seated cervical lymph nodes. The other models including the breast cancer model and the inguinal model in dog and the inguinal model and the small bowel model in pig can be used for sentinel node mapping experiment, but movement of tracers beyond the sentinel node could not be assessed with these models due to deep seated large sized lymph nodes. The capability of chasing lymphatic flows in NIR imaging system is believed to be helpful for patient with dark skin, and for detecting the unusual pathway of lymphatic flows which was shown in our experiment of pig that the ICG injected around the uppermost nipple travelled not to the adjacent lymph node but to the inguinal lymph node or the lowest breast located more than 45cm distally in two cases.

Compared with gastrointestinal tract including the small bowel and the stomach, relatively larger amount of tracer seemed to be useful to identify the lymphatic flows in cutaneous models, considering longer cutaneous lymphatic flows and need for brighter signal to penetrate skin. The least amount that enabled sentinel node identification in all three cutaneous models (breast in

pig, inguinal in dog and pig) was 0.2mg. In the gastric cancer model, the concentration of ICG commonly used in vital dye method was too high for the NIR imaging system in this experiments of gastric cancer model as well as in recent reports in human gastric cancer, because rapid dispersion of ICG and high sensitivity of NIR system resulted in identification of too many lymph nodes including lymph nodes beyond the sentinel lymph nodes as well. [23,50]

With ICG in lower concentration (0.1mg/ml), visibility of lymphatic system was far superior to that with 5mg/ml ICG inspected by naked eyes in the gastric model. However, ICG spread widely to multi-directionally and beyond the first draining lymph node in both canine and porcine stomach models. Nevertheless, ICG could be clinically applied because it showed not only the lymph nodes but also the lymphatic channel to among the injection site and lymph nodes, which could help the surgeon differentiating the first draining lymph nodes from the lymph nodes beyond.

ICG/ɣ-PGA complex was previously reported to superior to free ICG in terms of brightness and retention time in small animal models, however, it did not show clinically meaningful differences from single use of ICG in terms of signal intensity or dispersion characteristics in the large animal models in this study. One possible explanation might be that the lymphatic system around the gastrointestinal tract may have much abundant lipoproteins or albumin to which ICG bind with high affinity resulting in similar effect of ICG/ɣ-PGA complex that was observed in lymphatic channel of mice models.[51] This hypothesis also explains sustained signal as long as 2 days after the injection with single usage of ICG which signal intensity is rapidly diminishing and depleted within 24 hours *in vitro* due to aggregation and photobleaching.[32,38] This phenomenon led us to apply ICG in a marking method around the early gastric cancer by endoscopic injection 1 or 2 days before the operation in the later part of this study.

In contrast to ICG or ICG/ɣ-PGA complex, which showed multiple sentinel nodes and lymph nodes beyond them, NIR-PNG showed only one sentinel lymph node in the gastric cancer model in a dog and pigs. NIR-PNG did not showed any signal beyond the first node, and the injection site was relatively small and well margined round shape without out-spreading spikes. For the sensitivity's sake, smaller number of sentinel lymph node cannot be advantageous for sentinel lymph node biopsy.[52] Therefore we injected 5mg/ml of ICG at the same site as that of NIR-PNG in pigs to examine false-negative lymph nodes that could be missed by NIR-PNG. Even though more lymph node were found in different lymphatic flows to lesser curvature side and beyond the lymph node identified by NIR-PNG, no more node were identified between the injection sited and the first found lymph node by NIR-PNG. Whether less spreading features at the injection site of NIR-PNG will be helpful to increase specificity or disadvantageous to decrease sensitivity should be re-evaluated in human trial, because of the limitation of differences in the structures of the lymphatic system between animals and human.

The retention time was evaluated 1 week after injection of tracers in dogs because we found that the signal of ICG and ICG/ɣ-PGA complex also remains until 2 days after injection. The longer retention time of the signal of NIR-PNG in the injection site and only one lymph node identified at the first experiment as long as 1 week showed that NIR-PNG could be used as a better tracer for the sentinel lymph node biopsy with superior specificity and more liberal range of period for the endoscopic injection before surgery. A recent human application was reported that the number of lymph nodes identified by NIR system using ICG decreased compared with intraopertive injection when endoscopically injected 1-3 days before.[23] This method can be a clinically useful option, however, we expect that NIR-PNG could provide more

consistent number and location of sentinel lymph node regardless of the injection timing.

Previous studies showed that endoscopic injection is similar of superior to subserosal injection from outside stomach because of frequent leakage of the tracer to contaminate the field for sentinel lymph node biopsy.[34,53,54] Endoscopic injection can also develop the leakage of the tracers if the needle accidently punctures the stomach wall. However, the depth of injection can be monitored in intraoperative injection, and if the tracers are injected a few days before surgery, the tracer in the free peritoneal cavity seems to be washed out because all the tracers in this study are water-soluble. We also experienced of a leakage of ICG during the endoscopic injection, but the signal in the peritoneal cavity disappeared in an observation 2 days later.

One of the limitations of this study was that the lymphatic structure of the dogs and pigs was different from that of human stomach. While the sentinel lymph nodes were frequently found near the injection site in human stomach, the identified lymph nodes were located in relatively far area such as infrapyloric or suprapancreatic area in animal models in this study. Individual variation of the lymphatic was also difficult to develop consistent animal model for evaluation of tracers as seen in the case of breast cancer model in which the tracer moved to inguinal lymph nodes. We found that the greater curvature side of the lower body of the stomach was one of the best sites to assess the movement of tracers with the least effect of individual variation, which resulted in a limitation of numbers of examinations for statistical evaluation because it allowed only one test for one gastric cancer model. However, we expect that the characteristic information of each tracer obtained from this study will provide great help for the application of sentinel lymph node biopsy using NIR imaging system in human trial.

In summary, we have validated the high sensitivity and feasibility in clinical use of our own-made NIR imaging system in large animal model. The breast cancer model in pig was found to be not a good model, but inguinal cutaneous malignancy model in pig and breast cancer model and inguinal model in dog showed highly visible signal of dermal lymphatic flows as well as deep seated lymph nodes by newly developed tracers and NIR imaging systems. Together with these models, the small bowel model in pig could be a good model for gastrointestinal system, but all of these models could not assess the movement of the tracers beyond the sentinel lymph nodes. A gastric cancer model to examine the movement of tracers from the lower body greater curvature side of the stomach via the infrapyloric nodes and to suprapancreatic nodes was useful to assess lymphatic flows after the sentinel nodes. Among three tracers, NIR-PNG was found to be the best candidate for the sentinel lymph node biopsy in gastric cancer with distinct characteristics of long-standing retention in the sentinel lymph nodes specifically. In spite of disadvantage of quick dispersion, ICG also could be utilized for clinical application with diluted optimal dosages, because it showed highly sensitive visualization of not only the lymph nodes but also lymphatic flows, which help surgeon identifying the sentinel lymph nodes among the signalized lymph nodes.

CHAPTER 3

Marking of the location of gastric cancer using NIR fluorophores

INTRODUCTION

During the present studies, high penetration depth and prolonged retention time in injected sites of ICG was observed in NIR imaging system. These characteristics could be utilized for a method to mark the location of early gastric cancer which is difficult to be identified in surgery. The method is expected to be used for many patients considering recent increasing proportion of early staged gastric cancer detected by screening endoscopy and increasing application of intracorporeal anastomosis method in which the identification of the tumor location is essential to decide adequate resection line of the stomach.[55,56]

Because ICG showed relatively large size in previous studies and has a possibility to be washed out quickly, mixture of hyaluronic acid was considered, because it is used for the elongation of time of submucosal elevation during endoscopic resection.[57,58]

The purpose of this preliminary study is to examine that the ICG and hyaluronic acid mixture can be feasible to be used in marking methods for early gastric cancer by endoscopic injection a few days ago and intraoperatively inspected by NIR imaging systems.

MATERIALS AND METHODS

1. ICG and ICG mixed with hyaluronic acid

ICG in 0.1mg/ml was mixed with different concentration of hyaluronic acid (Mw 3,000kDa, LG life sciences Ltd., Seoul, Korea)

2. Inspection of the gastric injection site of tracers 2 days later

To assess the feasibility of a marking method by endoscopic injection 1-2 days before an operation, 0.5ml of ICG (0.1mg/ml) and NIR-PNG was injected endoscopically in the porcine stomach and the injection sites were marked by prolene suture. The injection sites were re-explored 2 days later.

3. *Ex vivo* injection of ICG, ICG/ɣ-PGA complex, and ICG + Hyaluronic acid

To examine the effect of additive viscous compounds to reduce the size of the marking signal of ICG, different concentration of ɣ-PGA and hyaluronic acid was mixed with 0.1mg/ml of ICG. Then 0.1 and 0.2ml of the mixtures were injected in the submucosal layer of the porcine stomach by 25 gauge needle, right after the stomach was removed from the living pig under general anesthesia. The stomach was flipped and the size of the fluorescence signal was calculated from the serosal side with the NIR camera system by the formula of (longest diameter + smallest diameter perpendicular to longest diameter)/2 (cm).

4. *In vivo* injection of ICG and ICG + Hyaluronic acid for marking of gastric lesions

To evaluate the retention property of the ICG (0.1mg/ml) mixed with different concentration of hyaluronic acid (0.025, 0.05, 0.1 and 0.2%), 0.1% of the mixtures were injected in the small bowel wall subserosally, and the travelling patterns were observed. The mixtures (0.2ml) were also injected in

the submucosal layer of the stomach by endoscopy, and the injection sites were inspected 2 days later.

RESULTS

1. Inspection of the gastric injection site of tracers 2 days later

When we inspect the injection site of ICG (0.1mg/ml) and NIR-PNG administered 2 days before endoscopically, the fluorescent signals remained bright with a longer diameter of 2.8cm and 2.0cm, respectively. (Figure 3-1) Based on this deep penetration of the fluorescent signals and longer duration of stay in the injection site of ICG, next experiments were designed to reduce the size of the signal and prolong the retention time using adjunctive viscous chemicals such as PGA and hyaluronic acid.

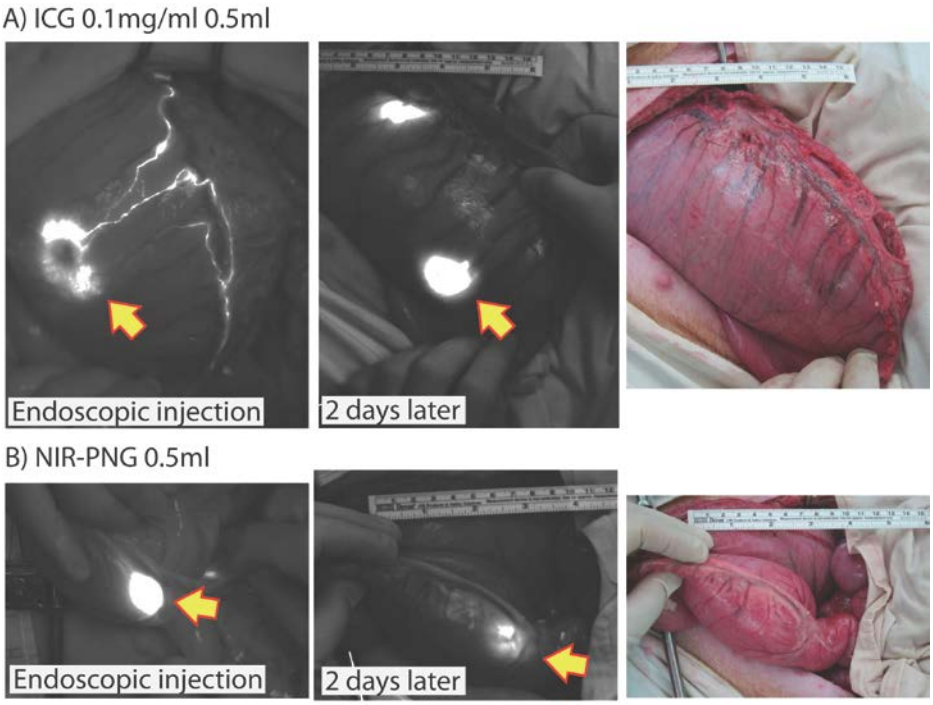

Figure 3-1. The fluorescent signal remained bright 2 days after endoscopic injection in the submucosal area of the stomach of pigs. A) 0.5ml of 0.1mg/ml ICG B) 0.5ml of NIR-PNG

2. *Ex vivo* injection of ICG, ICG/ɣ-PGA complex, and ICG + Hyaluronic acid

To exam the possibility to reduce the size of the wheals by tracer injection by adding viscous material, different concentrations of hyaluronic acid and ɣ-PGA were mixed with ICG and injected in the submucosal layer by 25 gauge needle. The fluorescent signals were very bright from the serosal side in the NIR image. The size of the signal of ICG + hyaluronic acid tended to smaller although we could not conclude a meaningful correlation between the size of a signal and the concentration of hyaluronic acid or ɣ-PGA. (Figure 3-2)

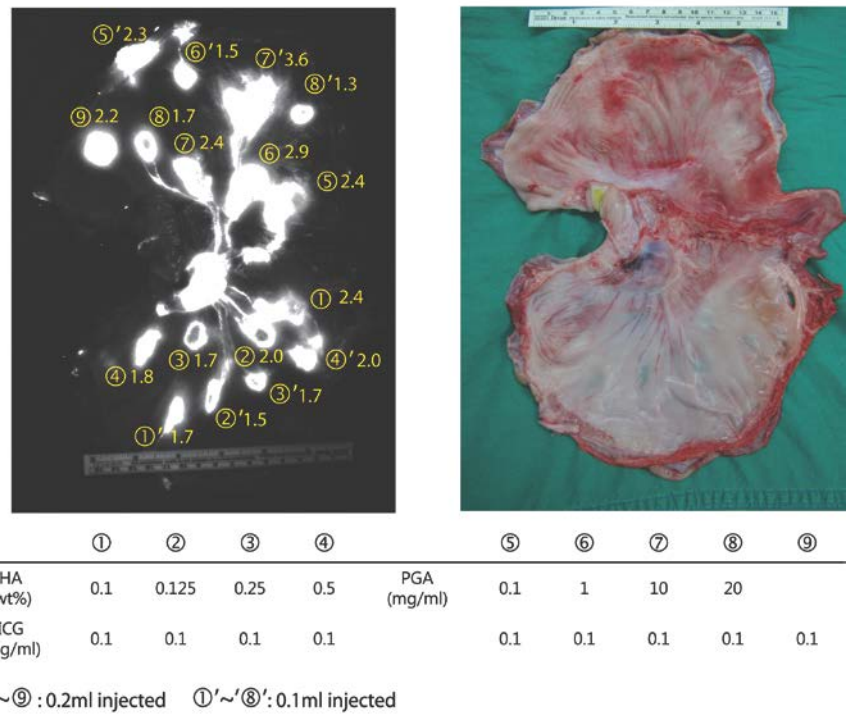

	①	②	③	④		⑤	⑥	⑦	⑧	⑨
HA (wt%)	0.1	0.125	0.25	0.5	PGA (mg/ml)	0.1	1	10	20	
ICG (mg/ml)	0.1	0.1	0.1	0.1		0.1	0.1	0.1	0.1	0.1

①~⑨ : 0.2ml injected ①′~′⑧′: 0.1ml injected

Figure 3-2. The average size of signal (cm) in NIR images from the serosal side of the stomach of the pig 17 minutes after the injection of tracers in the submucosal layer. Average size were calculated by (longest diameter + smallest diameter perpendicular to longest diameter)/2 (cm)

3. *In vivo* injection of ICG and ICG + Hyaluronic acid for marking of gastric lesions

Injection in the small bowel showed a tendency that the higher concentration of hyaluronic acid delays the movement of ICG from the injection site to the lymphatics (Figure 3-3) When injected in the stomach of the pig, the size of the signal tended to be smaller as the concentration of hyaluronic acid increase. All the marking sites by injection of ICG or mixture of ICG and ICG + hyaluronic acid could be clearly identified 2 days after the injection, which seems to be enough to indicate the location of the lesion in the stomach. (Figure 3-4) The reversed correlation between the size of the signal and concentration of hyaluronic acid was maintained 2 days after injection. Although the size of the signal was not so much different from each other considering clinical significance, the shape of mixture of ICG and hyaluronic acid remained spherical, while the signal of ICG had outspreading spikes.

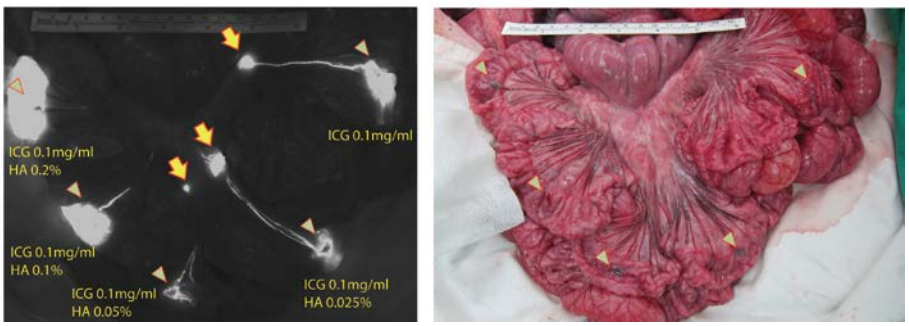

Figure 3-3. The signals in the small bowel and the mesenteric nodes after injection of ICG and mixtures of ICG+hyaluronic acid. Movement of ICG via lymphatics seemed to be delayed depending on the concentration of hyaluronic acid. Arrowhead: injection site, Arrow: sentinel lymph node

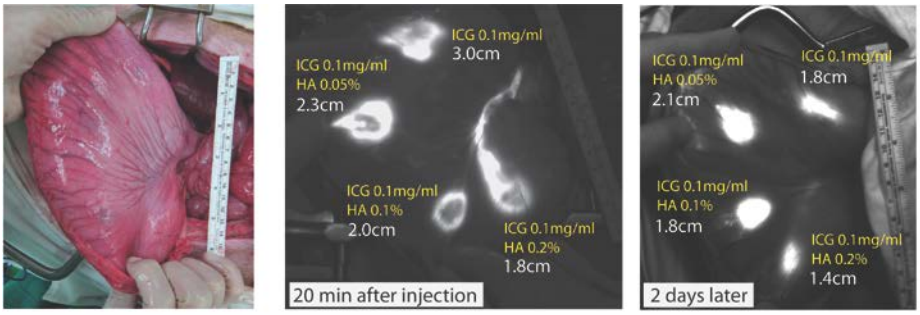

Figure 3-4. Bright signals of injection site of ICG and mixtures of ICG + hyaluronic acid 2 days after injection. The average size of signal were calculated by (longest diameter + smallest diameter perpendicular to longest diameter)/2 (cm)

DISCUSSION

As mentioned before, we applied the features of ICG which signal lasted a few days after injection with good tissue penetration to the marking method of early gastric cancer by endoscopic injection a few days before the operation. NIR-PNG also can be a good marker with long retention time and smaller and not-outspreading tendency at the injection sites. However, we examined the ICG and hyaluronic acid mixture because they are already used in the clinical practice and readily applicable to human trial for marking method with smaller risk of toxicity. It is expected that this method can be used in near future because a few successful laparoscopic NIR camera is ready to be commercialized.[50,59] Because the desired characteristic of tracer for marking is a tendency to be locally confined at the injection site with long retention time, hyaluronic acid could be a good adjunctive because it is used for the elongation of time of submucosal elevation during endoscopic resection.[57,58] ICG with higher concentration of hyaluronic acid showed a tendency of longer retention at the injection site in the small bowel of the pig as reported in previous study.[26] The size of the signal and the concentration of the hyaluronic acid also showed a reversed correlation in the stomach, however, the difference was minimal to be clinically meaningful and the differences of thickness of the stomach wall depending on the location might have affected results. The signal of ICG which was biggest at the time of injection became similar size with that of mixture of hyaluronic acid due to absence of the retention effect of hyaluronic acid. Therefore, ICG could be solely used for the marking method, but adding of hyaluronic acid may provide more security with longer retention time and more round shape marking because it is expected that the change of the size of ICG would be greater than mixture of hyaluronic acid depending on the time after injection.

In this study, we only focused on the characteristic of tracers for retention in injection site. Further studies using different tracers including NIR-PNG could identify better candidates which are useful in both marking and sentinel node mapping.

In summary, we identified some feasibility of the endoscopic injection of ICG or ICG and hyaluronic acid mixture to provide visible marking for early gastric cancer.

REFERENCES

1. Noh YW, Kong SH, Choi DY, et al. Near-Infrared Emitting Polymer Nanogels for Efficient Sentinel Lymph Node Mapping. *ACS nano.* 2012.
2. Moon HG, Han W, Noh DY. Comparable survival between pN0 breast cancer patients undergoing sentinel node biopsy and extensive axillary dissection: a report from the Korean Breast Cancer Society. *Journal of clinical oncology : official journal of the American Society of Clinical Oncology.* 2010;28:1692-1699.
3. Wong SL, Balch CM, Hurley P, et al. Sentinel Lymph Node Biopsy for Melanoma: American Society of Clinical Oncology and Society of Surgical Oncology Joint Clinical Practice Guideline. *Journal of clinical oncology : official journal of the American Society of Clinical Oncology.* 2012.
4. Miyashiro I. What is the problem in clinical application of sentinel node concept to gastric cancer surgery? *Journal of gastric cancer.* 2012;12:7-12.
5. Miwa K, Kinami S, Taniguchi K, et al. Mapping sentinel nodes in patients with early-stage gastric carcinoma. *The British journal of surgery.* 2003;90:178-182.
6. Park DJ, Lee HJ, Lee HS, et al. Sentinel node biopsy for cT1 and cT2a gastric cancer. *European journal of surgical oncology : the journal of the European Society of Surgical Oncology and the British Association of Surgical Oncology.* 2006;32:48-54.
7. Hayashi H, Ochiai T, Mori M, et al. Sentinel lymph node mapping for gastric cancer using a dual procedure with dye- and gamma probe-guided techniques. *Journal of the American College of Surgeons.* 2003;196:68-74.
8. Kitagawa Y, Fujii H, Mukai M, et al. Radio-guided sentinel node detection for gastric cancer. *The British journal of surgery.* 2002;89:604-608.

9. Tonouchi H, Mohri Y, Tanaka K, et al. Laparoscopic lymphatic mapping and sentinel node biopsies for early-stage gastric cancer: the cause of false negativity. *World journal of surgery.* 2005;29:418-421.
10. Frangioni JV. In vivo near-infrared fluorescence imaging. *Current opinion in chemical biology.* 2003;7:626-634.
11. Rao J, Dragulescu-Andrasi A, Yao H. Fluorescence imaging in vivo: recent advances. *Current opinion in biotechnology.* 2007;18:17-25.
12. Kitai T, Inomoto T, Miwa M, et al. Fluorescence navigation with indocyanine green for detecting sentinel lymph nodes in breast cancer. *Breast Cancer.* 2005;12:211-215.
13. Troyan SL, Kianzad V, Gibbs-Strauss SL, et al. The FLARE intraoperative near-infrared fluorescence imaging system: a first-in-human clinical trial in breast cancer sentinel lymph node mapping. *Annals of surgical oncology.* 2009;16:2943-2952.
14. Tagaya N, Aoyagi H, Nakagawa A, et al. A novel approach for sentinel lymph node identification using fluorescence imaging and image overlay navigation surgery in patients with breast cancer. *World journal of surgery.* 2011;35:154-158.
15. Noura S, Ohue M, Seki Y, et al. Feasibility of a lateral region sentinel node biopsy of lower rectal cancer guided by indocyanine green using a near-infrared camera system. *Annals of surgical oncology.* 2010;17:144-151.
16. Hirche C, Mohr Z, Kneif S, et al. Ultrastaging of colon cancer by sentinel node biopsy using fluorescence navigation with indocyanine green. *International journal of colorectal disease.* 2012;27:319-324.
17. Crane LM, Themelis G, Pleijhuis RG, et al. Intraoperative multispectral fluorescence imaging for the detection of the sentinel lymph node in cervical cancer: a novel concept. *Molecular imaging and biology : MIB : the official publication of the Academy of Molecular Imaging.* 2011;13:1043-1049.

18. Iga AM, Robertson JH, Winslet MC, et al. Clinical potential of quantum dots. *Journal of biomedicine & biotechnology.* 2007;2007:76087.
19. Kim S, Lim YT, Soltesz EG, et al. Near-infrared fluorescent type II quantum dots for sentinel lymph node mapping. *Nature biotechnology.* 2004;22:93-97.
20. Buckle T, Chin PT, van Leeuwen FW. (Non-targeted) radioactive/fluorescent nanoparticles and their potential in combined pre- and intraoperative imaging during sentinel lymph node resection. *Nanotechnology.* 2010;21:482001.
21. Pons T, Pic E, Lequeux N, et al. Cadmium-free CuInS2/ZnS quantum dots for sentinel lymph node imaging with reduced toxicity. *ACS nano.* 2010;4:2531-2538.
22. Benson RC, Kues HA. Fluorescence properties of indocyanine green as related to angiography. *Physics in medicine and biology.* 1978;23:159-163.
23. Yoshida M, Kubota K, Kuroda J, et al. Indocyanine green injection for detecting sentinel nodes using color fluorescence camera in the laparoscopy-assisted gastrectomy. *Journal of gastroenterology and hepatology.* 2012;27 Suppl 3:29-33.
24. Moody ED, Viskari PJ, Colyer CL. Non-covalent labeling of human serum albumin with indocyanine green: a study by capillary electrophoresis with diode laser-induced fluorescence detection. *Journal of chromatography B, Biomedical sciences and applications.* 1999;729:55-64.
25. Ohnishi S, Lomnes SJ, Laurence RG, et al. Organic alternatives to quantum dots for intraoperative near-infrared fluorescent sentinel lymph node mapping. *Molecular imaging.* 2005;4:172-181.
26. Kitayama J, Ishigami H, Ishikawa M, et al. Hyaluronic acid is a useful tool for intraoperative sentinel node detection in gastric cancer surgery. *Surgery.* 2007;141:815-820.

27. Noh YW, Park HS, Sung MH, et al. Enhancement of the photostability and retention time of indocyanine green in sentinel lymph node mapping by anionic polyelectrolytes. *Biomaterials.* 2011;32:6551-6557.
28. Henze E, Schelbert HR, Collins JD, et al. Lymphoscintigraphy with Tc-99m-labeled dextran. *Journal of nuclear medicine : official publication, Society of Nuclear Medicine.* 1982;23:923-929.
29. Saxena V, Sadoqi M, Shao J. Polymeric nanoparticulate delivery system for Indocyanine green: biodistribution in healthy mice. *International journal of pharmaceutics.* 2006;308:200-204.
30. Proulx ST, Luciani P, Derzsi S, et al. Quantitative imaging of lymphatic function with liposomal indocyanine green. *Cancer research.* 2010;70:7053-7062.
31. Cheng KC, Demirci A, Catchmark JM. Pullulan: biosynthesis, production, and applications. *Applied microbiology and biotechnology*. 2011;92:29-44.
32. Miyashiro I, Miyoshi N, Hiratsuka M, et al. Detection of sentinel node in gastric cancer surgery by indocyanine green fluorescence imaging: comparison with infrared imaging. *Annals of surgical oncology*. 2008;15:1640-1643.
33. Kusano M, Tajima Y, Yamazaki K, et al. Sentinel node mapping guided by indocyanine green fluorescence imaging: a new method for sentinel node navigation surgery in gastrointestinal cancer. *Digestive surgery*. 2008;25:103-108.
34. Tajima Y, Yamazaki K, Masuda Y, et al. Sentinel node mapping guided by indocyanine green fluorescence imaging in gastric cancer. *Annals of surgery.* 2009;249:58-62.
35. Akao T, Kimura T, Hirofuji YS, et al. A poly(gamma-glutamic acid)-amphiphile complex as a novel nanovehicle for drug delivery system. *Journal of drug targeting.* 2010;18:550-556.
36. Lee EH, Kamigaito Y, Tsujimoto T, et al. Synthesis of an amphiphilic poly(gamma-glutamic acid)-cholesterol conjugate and its application

as an artificial chaperone. *Journal of microbiology and biotechnology*. 2010;20:1424-1429.

37. Park do J, Kim HH, Park YS, et al. Simultaneous indocyanine green and (99m)Tc-antimony sulfur colloid-guided laparoscopic sentinel basin dissection for gastric cancer. *Annals of surgical oncology*. 2011;18:160-165.
38. Tajima Y, Murakami M, Yamazaki K, et al. Sentinel node mapping guided by indocyanine green fluorescence imaging during laparoscopic surgery in gastric cancer. *Annals of surgical oncology*. 2010;17:1787-1793.
39. Cimmino VM, Brown AC, Szocik JF, et al. Allergic reactions to isosulfan blue during sentinel node biopsy--a common event. *Surgery*. 2001;130:439-442.
40. Zhuang X, Ha T, Kim HD, et al. Fluorescence quenching: A tool for single-molecule protein-folding study. *Proceedings of the National Academy of Sciences of the United States of America*. 2000;97:14241-14244.
41. Weinberg J, Greaney EM. Identification of regional lymph nodes by means of a vital staining dye during surgery of gastric cancer. *Surgery, gynecology & obstetrics*. 1950;90:561-567.
42. Cox KR, Hare WS, Bruce PT. Lymphography in melanoma. Correlation of radiology with pathology. *Cancer*. 1966;19:637-647.
43. Abbes M. Experience with lymphangiography in the surgical management of breast cancer. *International surgery*. 1967;47:243-245.
44. Abbes M, Juillard G, Giraud C. [Lymph node extensions of urogenital cancers in men (use of lymphography apropos of 73 cases)]. *Journal d'urologie et de nephrologie*. 1967;73:547-556.
45. Morton DL, Wen DR, Wong JH, et al. Technical details of intraoperative lymphatic mapping for early stage melanoma. *Archives of surgery*. 1992;127:392-399.
46. Krag DN, Anderson SJ, Julian TB, et al. Sentinel-lymph-node resection compared with conventional axillary-lymph-node dissection

in clinically node-negative patients with breast cancer: overall survival findings from the NSABP B-32 randomised phase 3 trial. *The lancet oncology*. 2010;11:927-933.

47. Wong SL, Balch CM, Hurley P, et al. Sentinel lymph node biopsy for melanoma: American Society of Clinical Oncology and Society of Surgical Oncology joint clinical practice guideline. *Journal of clinical oncology : official journal of the American Society of Clinical Oncology*. 2012;30:2912-2918.
48. Namikawa K, Yamazaki N. Sentinel lymph node biopsy guided by indocyanine green fluorescence for cutaneous melanoma. *European journal of dermatology : EJD*. 2011;21:184-190.
49. Tsujino Y, Mizumoto K, Matsuzaka Y, et al. Fluorescence navigation with indocyanine green for detecting sentinel nodes in extramammary Paget's disease and squamous cell carcinoma. *The Journal of dermatology*. 2009;36:90-94.
50. Miyashiro I, Kishi K, Yano M, et al. Laparoscopic detection of sentinel node in gastric cancer surgery by indocyanine green fluorescence imaging. *Surgical endoscopy*. 2011;25:1672-1676.
51. Yoneya S, Saito T, Komatsu Y, et al. Binding properties of indocyanine green in human blood. *Investigative ophthalmology & visual science*. 1998;39:1286-1290.
52. Ryu KW, Eom BW, Nam BH, et al. Is the sentinel node biopsy clinically applicable for limited lymphadenectomy and modified gastric resection in gastric cancer? A meta-analysis of feasibility studies. *Journal of surgical oncology*. 2011;104:578-584.
53. Yaguchi Y, Ichikura T, Ono S, et al. How should tracers be injected to detect for sentinel nodes in gastric cancer--submucosally from inside or subserosally from outside of the stomach? *Journal of experimental & clinical cancer research : CR*. 2008;27:79.
54. Lee JH, Ryu KW, Kim CG, et al. Comparative study of the subserosal versus submucosal dye injection method for sentinel node biopsy in gastric cancer. *European journal of surgical oncology : the journal of*

the European Society of Surgical Oncology and the British Association of Surgical Oncology. 2005;31:965-968.

55. Kanaya S, Gomi T, Momoi H, et al. Delta-shaped anastomosis in totally laparoscopic Billroth I gastrectomy: new technique of intraabdominal gastroduodenostomy. *Journal of the American College of Surgeons.* 2002;195:284-287.

56. Bouras G, Lee SW, Nomura E, et al. Surgical outcomes from laparoscopic distal gastrectomy and Roux-en-Y reconstruction: evolution in a totally intracorporeal technique. *Surgical laparoscopy, endoscopy & percutaneous techniques.* 2011;21:37-41.

57. Hirasaki S, Kozu T, Yamamoto H, et al. Usefulness and safety of 0.4% sodium hyaluronate solution as a submucosal fluid "cushion" for endoscopic resection of colorectal mucosal neoplasms: a prospective multi-center open-label trial. *BMC gastroenterology.* 2009;9:1.

58. Yoshida N, Naito Y, Kugai M, et al. Efficacy of hyaluronic acid in endoscopic mucosal resection of colorectal tumors. *Journal of gastroenterology and hepatology.* 2011;26:286-291.

59. Cahill RA, Anderson M, Wang LM, et al. Near-infrared (NIR) laparoscopy for intraoperative lymphatic road-mapping and sentinel node identification during definitive surgical resection of early-stage colorectal neoplasia. *Surgical endoscopy.* 2012;26:197-204.

국문 초록

서론: 근적외선 촬영 시스템은 현재의 감시림프절 생검 방법의 문제점들을 극복할 수 있는 새로운 방법으로 제시되었다. 이 연구의 목적은 대동물 모델을 이용하여 자체적으로 제작한 근적외선 촬영 장치의 활용 가능성을 확인하고 대동물에서의 유방, 흑색종, 소장 및 위암 모델을 개발, 검증하며, 인도시아닌 그린의 단점을 보완할 수 있는 새로운 표지자를 개발하여 대동물에서 확인하는 것이다.

방법: 인도시아닌 그린(ICG)의 적절 농도를 돼지의 소장과 위에 주입하여 확인하고, 근적외선염료 IRDye900 이 결합된 플루란-콜레스테롤 나노표지자 (NIR-PNG)를 개발하고 특성을 확인하였다. 40kg 의 돼지와 30kg 의 개를 이용하여 유방암, 피부암, 소장 및 위암 모델을 준비하고, 인도시아닌 그린(ICG), ICG/폴리감마글루타민산 (ICG/PGA) 복합체, ICG/히알우론산(ICG/HA) 혼합물, 근적외선염료 IRDye900 이 결합된 플루란-콜레스테롤 나노표지자 (NIR-PNG) 등을 여러 농도와 양으로 주입하여 민감도, 표지자 확산 양상, 잔류 시간 등 표지자들의 특성을 비교해 보았다.

결과: 위장관의 감시림프절 생검을 위한 ICG 의 적절 농도는 0.1-1mg/ml 이었고 NIR-PNG 는 IRDye800 에 비해 림프절에서 더 밝고 오래 잔류하였다. 근적외선 촬영법은 유방암과 피부암 모델에서 림프절뿐 아니라 피부의 림프관 흐름을 잘 보여줄 정도로 예민하였다. ICG 와 ICG/PGA 복합체는 위암모델에서 0.1mg/ml 의

농도로 주입되었을 때, 육안적 관찰을 위해 사용되는 5mg/ml 의 ICG 보다 더 예민한 가시성을 보여 주었으나, 여러 방향으로 확산되어 많은 림프절로 이동하였다. 반면 NIR-PNG 는 한 개의 감시림프절로만 이동하였고 더 오래 잔류하였다. ICG 와 ICG/HA 혼합물은 내시경으로 주입하였을 때 조기 위암의 위 절제 범위 결정을 위한 위치 표시 방법으로서의 사용 가능성을 보여 주었다.

결론: 근적외선 촬영시스템은 여러 가지 암종의 감시림프절 생검에서 높은 가시성을 제공하는 방법으로 사용될 수 있을 것으로 보인다. NIR-PNG 는 감시림프절에만 이동하여 머무는 좋은 표지자로 사용될 수 있을 것으로 기대되며, 적정 농도로 희석된 ICG 도 림프절뿐 아니라 림프관의 흐름을 잘 보여주는 예민한 표지자로 위암에서 근적외선 촬영시스템을 통해 사용될 수 있을 것이다.

* 본 내용중 NIR-PNG 의 개발에 관한 내용은 ACS Nano 학술지 (Noh YW, Kong SH (co-first author), Choi DY, et al. Near-infrared emitting polymer nanogels for efficient sentinel lymph node mapping. ACS Nano. 2012 Sep 25;6(9):7820-31)에 출판 완료된 내용임

주요어 :감시림프절생검, 근적외선촬영, 대동물모델

학 번 : 2009-30497

감사의 글

수월하게 적은 수의 동물실험으로 결과를 도출할 것으로 기대하고 시작했던 실험은 항상 예상을 벗어나는 대동물 실험의 결과와 구제역 등의 어려움으로 2 년 3 개월동안 20 마리의 돼지와 5 마리의 개를 사용해서야 어느 정도 정리가 될 수 있었습니다. 근적외선 카메라시스템과 새로운 표지자 기술을 선도하는 충남대 임용택 교수님 팀과 함께 모범적인 연구 협력을 가능케 해 주신 김희찬 교수님 강건욱 교수님과, 더불어 연구 진행 내내 좋은 아이디어와 격려를 아끼지 않으신 지도교수 양한광 교수님 및 이혁준 교수님 등 연구를 지도해 주신 모든 선생님들께 진심 어린 감사의 말씀을 드립니다. 무엇보다 임용택 교수님의 전폭적인 지원 하에 충남대에서 서울까지 매번 대동물 실험이 있을 때마다 먼 길을 달려 오셔서 식사도 거르면서 함께 헌신적으로 협력하여 주신 노영욱 박사님과 박혜선 연구원이 없었다면 연구는 진행될 수 없었을 것입니다. 대동물 실험은 단순한 결과를 얻기 위해서도 상당한 수고가 따르는 일이었습니다. 동물 반입과 사육, 실험을 위한 마취와 실험 후 관리를 도와준 김사훈 수의사와 최영락씨를 비롯한 모든 동물실험실 직원분들께 감사를 드립니다. 또한 대동물 실험을 위한 수술 준비, 동물 이송, 마취 및 수술, 내시경 시술, 수술 후 정리 및 청소에 이르기까지 많은 일에 서울대병원 외과 전임의로서 큰 도움을 준 서윤석, 한동석, 이경구, 오승영, 권창모 선생님들에게 진심으로 감사드리며, 일손이 부족할 때 근적외선 카메라와 조직 샘플 관리 등을 도와준 서울대병원 종양생물학 박사과정의 한태수, 유지은, 최보람, 이지연 학생들도 큰 힘이 되어

주었습니다. 실험 초기 여러 가지 공학적인 아이디어를 제공하였던 의공학과 김선권 연구원, 동물 실험과 조직 처리에 도움을 주었던 핵의학과 김영화 연구원과 의공학과 류지원 연구원에게도 감사의 말씀을 드립니다.